UNCLASSIFIED

AD NUMBER

AD817832

NEW LIMITATION CHANGE

TO

Approved for public release, distribution unlimited

FROM

Distribution authorized to U.S. Gov't. agencies only; Administrative/Operational Use; AUG 1966. Other requests shall be referred to Federal Aviation Agency, Attn: Director of Supersonic Transport Development, Washington, DC, 20553.

AUTHORITY

FAA, per DTIC Form 55, 21 Oct 1991

THIS PAGE IS UNCLASSIFIED

AD817832

LOCKHEED CALIFORNIA COMPANY

A Division of Lockheed Aircraft Corporation

BURBANK, CALIFORNIA, U.S.A.

AD No.

DDC FILE COPY

DDC

AUG 4 1967

B

Best Available Copy

LOCKHEED · CALIFORNIA COMPANY
A DIVISION OF LOCKHEED AIRCRAFT CORPORATION

(11) 19 Aug 66

(12) 79p.

REPORT NO. (14) LR-[illegible] JN

DATE August 19, 1966

MODEL SST

COPY NO. ______

TITLE

(6) CORONA PREVENTION IN THE SST WIRING SYSTEM,

REFERENCE W.O. 71-1405-7342

CONTRACT NUMBER(S) ______

PREPARED BY R. S. Henning
(10) R. S. Henning

CHECKED BY E. B. Evans
E. B. Evans

APPROVED BY N C Clark
N. C. Clark, Electrical Systems Lab.

Engineering Only - APPROVED BY Fred Mintz
Fred Mintz, Manager
Vehicle Systems Laboratory

*Outside Agencies. - APPROVED BY B. D. O'Laughlin
B. D. O'Laughlin, Division Engineer
Rye Canyon Research Center

*Specific Approval Required

REVISIONS

REV. NO.	DATE	REV. BY	PAGES AFFECTED	REMARKS

FORM 402-2

(209970)

ccf

NOTICE

ABSTRACT

The high altitudes and temperatures associated with SST supersonic flight and the use of electrical power at 230/400 volts introduces the need for design precautions to avoid corona or sparkover. As part of the wiring development program, investigations including a literature search, data analysis, and laboratory tests were conducted to determine the precautions required.

An approach is presented which is intended to simplify the design for corona prevention.

Further investigation and confirming tests are still to be conducted.

TABLE OF CONTENTS

APPENDIX

LIST OF ILLUSTRATIONS

LIST OF TABLES

1.0 INTRODUCTION

It has long been established classically that for all gases there is a minimum voltage between electrodes below which electrical breakdown, in the form of an avalanche discharge resulting in corona or sparkover, cannot occur. For potentials above this minimum, determination of the voltage required for the onset of an avalanche discharge is based on the Paschen curve for the gas, modified to take into account non-uniform fields. The onset voltage is a function of the gas density and the width of the gap separating the electrodes, as well as other factors including the presence of insulation on the conductor or within the gap. The nature of electrical breakdown in air is discussed in more detail in Appendix A.

The 230/400 system voltage exceeds the minimum of the Paschen curve for air, and the reduced air density at the altitudes and temperatures associated with supersonic flight, as compared with subsonic, increases the spacings and insulation thickness required to prevent electrical discharges. These discharges can produce undesirable effects including insulation deterioration and electromagnetic interference.

The object of this investigation was to determine the design guidelines required to avoid these discharges without significant cost in weight or space requirements.

2.0 CONCLUSIONS

1. As discussed in 5.1.2 and 5.5.2.2, corona must be avoided because it transmits interference into electronic equipment and produces cumulative deterioration and erosion of insulation and other materials in proportion to the product of corona intensity and time; while sparkover is intolerable because it can cause immediate equipment damage and loss of circuit function.

2. Corona and sparkover can be prevented by:

   a. Avoiding contamination on surfaces of conductors and thin insulations.

   b. Selecting materials and dimensions that can withstand the worst-case voltage gradients around energized conductors.

   c. Elimination of short air gaps between thinly-insulated conductors.

   d. Selection of insulating materials with maximum resistivity and dielectric strength, and low dielectric constant.

   e. Application of the Paschen Law curve as modified for non-uniform fields.

   f. Basing all calculations on the instantaneous peak "abnormal overvoltage" of the system.

3. For the 230/400 nominal system voltage and the SST operating altitude and temperatures, weight and space requirements can be minimized by avoiding areas in which energized conductors, with or without insulation, can be adjacent to unpressurized air. For such areas particular attention must be directed toward providing adequate spacing and insulation thickness, as presented by the guidelines in this report.

4. Corona or arc-overs are most likely to start in the air portion of the space between conductors, not in the insulation. Prevention of air breakdown is therefore the prime consideration.

5. The breakdown of air is promoted by high voltage gradient; inability of electrons and ions to escape without ionizing or exciting other atoms in the air; by the presence of ultraviolet

light as from excited atoms of air in the gap; and other mechanisms (see Appendix A) producing emission of secondary electrons from the electrodes. Breakdown can therefore be minimized by:

a. Avoiding sharp points and edges on the conductors.

b. Assuming that the final configuration has at some point a gradient as high as for needle points.

c. Using an air breakdown strength (volts/mil) corresponding to the worst combination of ion entrapment and secondary emissions in the gap.

d. Designing for the maximum altitude and temperature to which the designated parts will be exposed.

6. As discussed in 6.4, desirable features of design to prevent electrical discharges are:

a. To completely enclose connectors and terminals.

b. To arrange that voltage gradients are from line-to-neutral rather than from line-to-line in 3-phase circuits.

c. To coat all conductor surfaces with dielectric material to prevent sparkover.

7. The occurrence of corona can best be precluded by taking advantage of design features that are also desirable from other considerations. These include:

a. The use of multiconductor cable for weight saving.

b. The use of sealed assemblies to prevent oxidation and to exclude moisture.

c. The provision of conductive coatings on insulation for shielding.

3.0 CONFIGURATIONS TESTED

Electrodes of rounded and pointed metal, insulated wires and titanium sheet in various configurations, as required to verify analysis or to extend the data available in the literature, were tested to determine the conditions that produce the onset of corona and flashover.

4.0 PROCEDURE

The literature listed under References was assembled with the assistance of the Lockheed Technical Information Center. This literature was studied, the available data was analyzed, confirming and supplementary tests were conducted, design guidelines were formulated to prevent electrical discharges including corona, and a follow-on effort was planned, as discussed herein.

5.0 RESULTS

5.1 Design Guidelines

5.1.1 Definition of Electrical Breakdown in a Gas

An electrical breakdown of a gas surrounding a set of electrodes is said to have occurred if each electron liberated by the cathode undergoes a sufficient number of inelastic interactions to produce one or more secondary electrons from the cathode due to products of these interactions (photons, ions, or excited molecules).

5.1.2 Effects of Electrical Discharges

Corona or electrical discharges within an electrical power system transmit interference into communication equipment and electronic circuits; ; they cause deterioration of insulation and conductors; and they produce ionized gases, ozone, and corrosive agents such as weak nitric acid from air and

moisture. Sparkover between bare electrodes results in currents limited only by the impedance of the power source and connecting lines, and by the circuit protection. Although some quantitative date is available, the effects of corona on the deterioration rate of materials is difficult to assess. For these reasons corona discharges are to be avoided, except perhaps for brief periods under rare abnormal conditions.

5.1.3 Basic Considerations

The fundamental nature of electrical breakdown between electrodes in air, and within voids in insulation is discussed in Appendix A. The effective presentation of practical design guidelines to avoid corona and sparkover effects must be based on theoretical analysis which is verified by experimental data. In general, the guidelines are based on the expression for breakdown in uniform fields, namely

$$\gamma \varepsilon^{\alpha\delta} = 1 \tag{1}$$

where α is the first Townsent coefficient or the number of ionizing collisions made by one electron drifting 1 cm in the direction of the field; and γ is the second Townsend coefficient or the number of secondary electrons produced at the cathode per electron produced in the gap by primary collisional ionization. The value of $\epsilon^{\alpha\delta}$ may be of the order of 10^7, while γ may be of the order of 10^{-4}. For nonuniform fields a more general expression applies, namely

$$\gamma \left[\exp \left(\int_0^{\delta} \alpha dx \right) - 1 \right] = 1 \tag{2}$$

An expression closely approximating the Paschen curve for uniform fields in air is

$$V_s = \frac{Bp\gamma}{\ln p\delta + \ln \left[\frac{A}{\ln (1 + 1/\gamma)} \right]} \tag{3}$$

where V_S is the breakdown potential; $A = 8.8\ cm^{-1}mmHg^{-1}$; $B = 256\ volts^{-1}\ cm \times mmHg$; γ is 4.9×10^{-4} (theoretically a variable reflecting cathode characteristics, but about constant for many practical cases with the notable exception of titanium); p is the pressure in mmHg, and δ is the gap in cm.

Compensation must be made for the voltage gradients around wires, insulation, and connectors. Small radii, especially in contact with air, are to be avoided. For the SST temperature-altitudes the minimum breakdown voltage (325 volts peak) occur at gaps in the order of 1 mm. Air gaps or voids, and insulation on conductors, should be treated as capacitors to determine voltage division; thus, a low dielectric constant for insulation is desirable. Insulation resistance may be a factor for some materials.

5.1.4 Paschen Curve Modified to Take Into Account Non-uniform Fields.

The Paschen curve for uniform fields is shown in Figure 1. Departure from uniform fields may reduce the discharge onset voltage. (Other analysis presented (Ref. 1) indicates that it also raises the onset voltage gradient.) On the same figure is shown a curve for point electrodes. Plotted on Figures 13, 14, 15, and 16 are data points for various electrodes from the literature and from the laboratory tests.

Simple, conservative design guidelines can be based on the minimum onset voltages shown in Figure 1, which gives 325 peak volts (230 rms) as the minimum sparking voltage for air at room temperature. Ref. 2 shows that this is the most frequently quoted value of minimum sparkover voltage, but other values were found that ranged from 345 peak volts to 275 peak volts. This lower value is believed to be an absolute minimum voltage below which sparkover cannot occur under any circumstances of external electrostatic and electromagnetic fields. SST environments will most likely require the use of 325 peak volts at this absolute minimum.

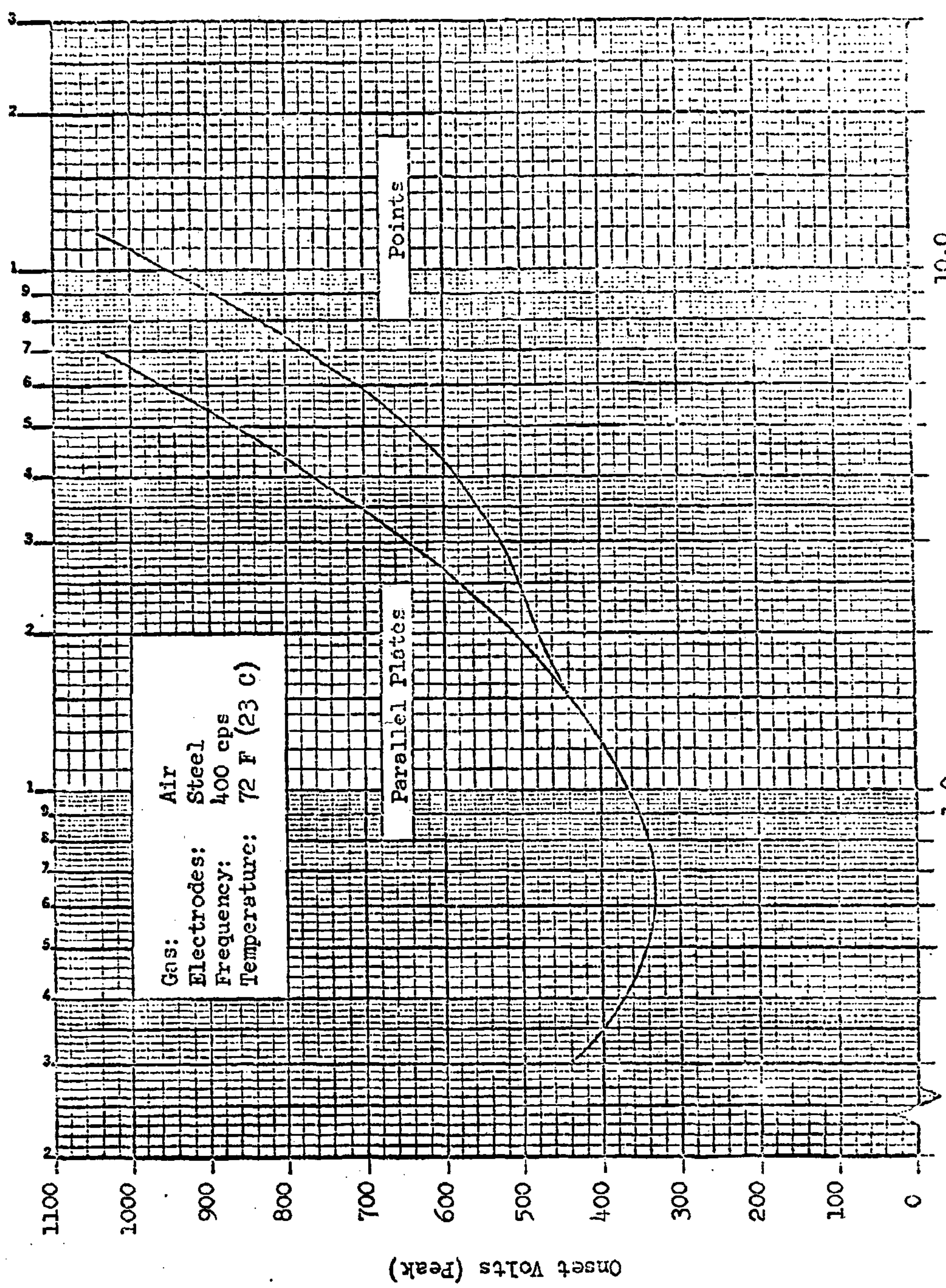

Figure 1 Paschen's Law Curve for Points and Parallel Plates (Ref. 15)

5.1.5 Practical Variation of Parameters

5.1.5.1 Electrode Shape - The Paschen curve holds only for uniform fields, but fields are frequently nonuniform in practice. Such fields are concentrated near small radii on the surfaces of the electrodes. Determination of the fields is a difficult mathematical process except for simple shapes like spheres or cylinders. Needle-points require resorting to field mapping using Teledeltos paper, equivalent uniform conductive films, or equivalent computer techniques.

In the case of nonuniform fields, reasoning presented in Ref. 1 indicates that, if the maximum field or voltage gradient does not exceed the uniform field (or voltage divided by gap) indicated by a point on the Paschen curve for given value of pδ (pressure in mmHg x gap in cm), then discharge onset will not occur. However, considering the difficulty of determining the fields in practical designs, a much simpler criterion, leading to a somewhat more conservative design, is suggested. The latter method is to avoid sharp radii, and to determine the required spacings and insulation thicknesses by reference to the curve on Figure 1 for needle points. Note that the curve for uniform fields (parallel plates properly contoured at the edges) and needle points coincide over much of the critical range of pδ.

For preliminary design purposes, it is considered that the Paschen curve (Figure 1) relating voltages between electrodes and pδ for uniform fields should be considered as a desirable condition and the curve for needle points as an undesirable condition.

5.1.5.2 Electrode Materials - Actually, the discharge onset voltage depends on the electrode materials, especially for the cathode. However, the literature indicates that, unless very careful control is exercised, surface contamination from exposure to normal atmosphere results. Thereafter, it is difficult to distinguish any difference in onset voltage for different materials. A notable exception may be titanium, which is an

excellent emitter of electrons at higher temperatures (see Ref. 3). The significance of this factor at SST temperatures is now being investigated further. It is indicated that this effect can be minimized by applying a coating of zicromium or a dielectric such as paint to the titanium. It should be noted that an electrode may be metal or insulating material. Pending further investigation, as noted above, it is considered that the effect of electrode material on the onset voltage can be ignored for preliminary design purposes.

5.1.5.3 Air Constituents - Actually, the discharge onset voltage varies for different gases and mixtures in the electrode gap. However, the literature (Ref. 4) indicates that atmospheric variations with altitude are not significant for preliminary design purposes. Ozone has an unevaluated effect, but wiring in the engine area will be protected from ozone, and the ozone concentrations in the other unconditioned areas will be relatively small.

Ref. 5 material indicates that humidity does not have a significant effect on discharge onset voltage unless water is condensed on the surfaces. Then, of course, moisture absorption and surface leakage are significant factors.

For the purposes of preliminary design, it is considered that atmospheric variations can be neglected, but wet insulation is very significant.

5.1.5.4 Frequency - The Ref. 6 is clear that frequency up to, and well beyond, that of a-c power system voltage does not influence the onset voltage for discharges.

5.1.6 Applicable Voltages, Temperatures, and Altitudes
The proposed SST a-c power generating system will operate at 230/400 rms volts with a nominal frequency of 400 cps. It will be a three-phase, 4-wire "Y" system with the neutral point of the source of power connected to ground, and thus a fourth conductor.

SST Spec. 422615 (Ref. 7) as shown in Figure 2, delineates the characteristics of electric power to be supplied by this generating system. It states that voltage transients, when converted to their evaluated step function loci (see MIL-STD-704, 6 October 1959, Section 7.6), shall be within the limits of Figure 2 for all operations of the aircraft generating system. The evaluated step function loci of the a-c voltage transients for all normal generating system operations are to be within the limits of 2 and 3 of Figure 2. For abnormal operation, the evaluated step function loci for a-c voltage transients are to be below limit 1.

It is noted at this point that SST Spec. 422615 is given for 230 rms volt operation and a conversion must be made to correspond to operation at 400 rms volts.

From Figure 2, the maximum abnormal overvoltage for 230 volt operation as dictated by limit 1 is 364 rms volts (515 volts peak). This corresponds to 364 (400/230) 634 rms volts (896 volts peak) for a system voltage of 400 rms volts.

From Figure 2 it is also seen that the maximum normal operating voltage for a 230 rms volt system is 300 volts rms (424 volts peak). This is equivalent to 522 rms volts (738 volts peak) for a 400 rms volt system voltage.

The maximum steady state normal operating voltage for a 230 rms volt system is 235 rms volts (332 volts peak). This corresponds to 408 rms volts (578 volts peak) for a 400 rms volt system.

It is thus dictated by SST Spec. 422615 that the maximum abnormal overvoltage for 400 rms volt line-to-line operation must not exceed 896 volts peak; the maximum abnormal overvoltage for 230 rms volt line-to-neutral operation must not exceed 515 volts peak; the maximum normal operating overvoltage

SST Spec. 422615 (Ref. 7) as shown in Figure 2, delineates the characterist of electric power to be supplied by this generating system. It states that voltage transients, when converted to their evaluated step function loci (see MIL-STD-704, 6 October 1959, Section 7.6), shall be within the limits of Figure 2 for all operations of the aircraft generating system. The evaluated step function loci of the a-c voltage transients for all normal generating system operations are to be within the limits of 2 and 3 of Figure 2. For abnormal operation, the evaluated step function loci for a-c voltage transients are to be below limit 1.

It is noted at this point that SST Spec. 422615 is given for 230 rms volt operation and a conversion must be made to correspond to operation at 400 rms volts.

From Figure 2, the maximum abnormal overvoltage for 230 volt operation as dictated by limit 1 is 364 rms volts (515 volts peak). This corresponds to 364 (400/230) 634 rms volts (896 volts peak) for a system voltage of 400 rms volts.

From Figure 2 it is also seen that the maximum normal operating voltage for a 230 rms volt system is 300 volts rms (424 volts peak). This is equivalent to 522 rms volts (738 volts peak) for a 400 rms volt system voltage.

The maximum steady state normal operating voltage for a 230 rms volt systen is 235 rms volts (332 volts peak). This corresponds to 408 rms volts (578 volts peak) for a 400 rms volt system.

It is thus dictated by SST Spec. 422615 that the maximum abnormal overvolta for 400 rms volt line-to-line operation must not exceed 896 volts peak; the maximum abnormal overvoltage for 230 rms volt line-to-neutral operation must not exceed 515 volts peak; the maximum normal operating overvoltage

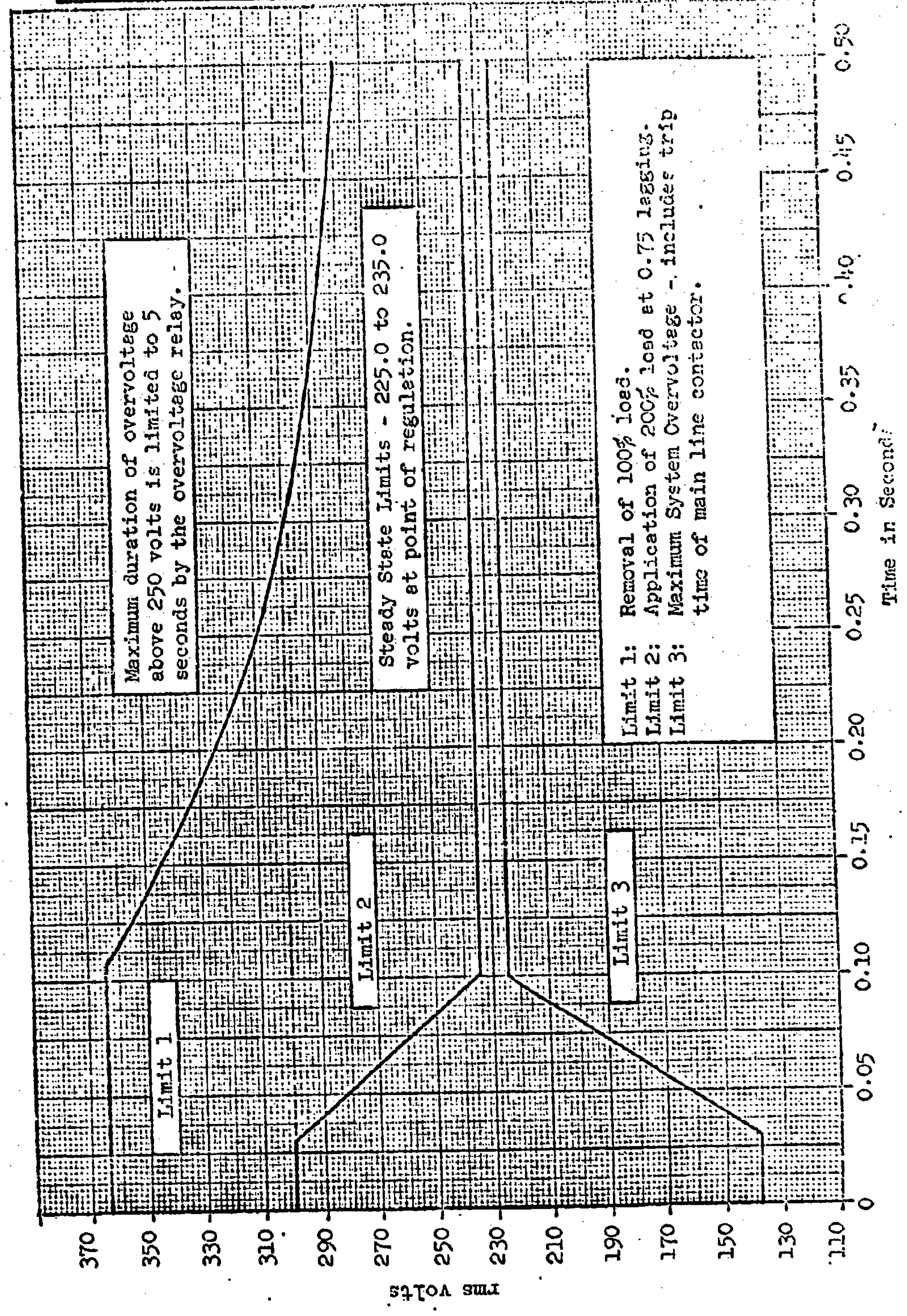

Figure 2 SST Spec. 422615, Transient, Steady State, and Overvoltage Limits

must not exceed 738 volts peak for 400 rms volt line-to-line operation; and the maximum normal operating overvoltage must not exceed 424 volts peak for 230 rms line-to-neutral operation. These values become very important when dictating electrode spacings and insulation thicknesses required for prevention of corona onset at SST altitudes and temperatures. Suppression techniques should be used to ensure that these peak values are never exceeded due to inductive switching.

Lockheed's L-2000 SST will operate up to 80,000 feet under a thermal environment as shown in Figure 3 for mach 2.7 cruise. Engine area wiring will function under an ambient temperature of 600 F to 800 F with a probable 100 F increase due to I^2R losses, or 700 F to 900 F total. Corona will not be a significant problem in this area due to "ram air" engine cooling which will increase air density and yield a larger value of $p\delta$ ($p\delta$ = 100 mmHg x cm at 47,000 feet for a 1 cm gap). Wing area wiring will function under a maximum ambient of 430 F or no higher than approximately 530 F when including I^2R losses. A complete analysis of thermal heating in a wire or multiconductor cable due to I^2R losses and high ambient temperatures is discussed in Lockheed Report 19868 (Ref. 8).

5.1.7 Analysis of Design Considerations

To simplify initial analysis, round-number approximations and simplifying assumptions will be used. Then a more exact detailed analysis can follow.

5.1.7.1 Applicable Data - The air density corresponding to the maximum operating altitude of 80,000 feet, and maximum harness operating temperature, assumed to be 600 F, is that corresponding to 100,000 feet at room temperature, or about 8.29 mmHg. Referring to the Paschen curve of Figure 1, the minimum onset voltage value is at about 0.65 mmHg x cm; or at about 0.79 mm (approximately 31 mils of an inch) spacing at 8.29 mmHg pressure. This is the air gap for minimum discharge onset voltage of about 325 peak volts.

LOCKHEED • CALIFORNIA COMPANY
A DIVISION OF LOCKHEED AIRCRAFT CORPORATION

REVISIONS ______ REPORT NO. 19306

PAGE NO. 13

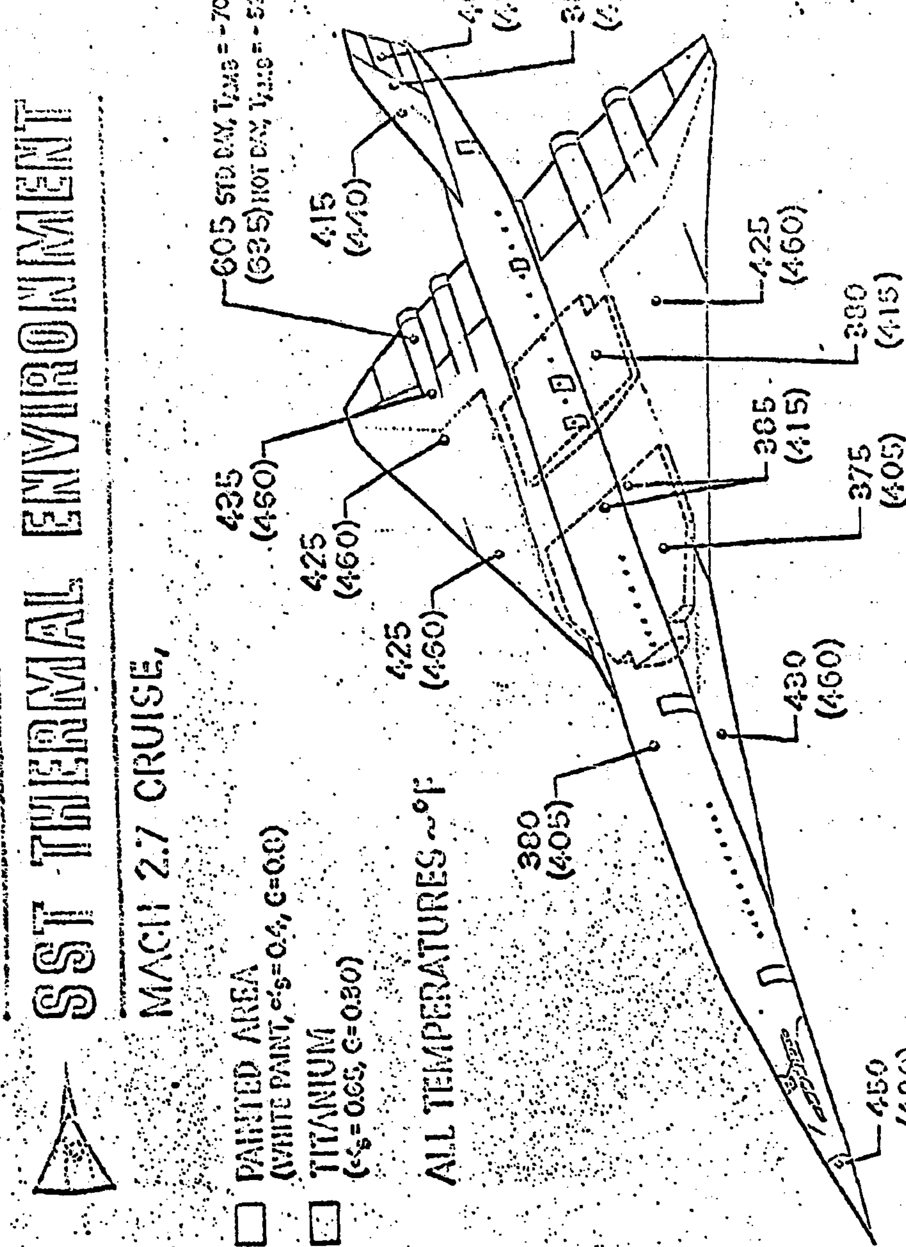

Figure 3 SST Thermal Environment

5.1.7.2 Conventional Wire Harness - Consider the conventional wire harness of past aircraft designs. Air gaps between insulated wires vary from zero to many times 31 mils. Whatever gaps between wires is required for minimum onset voltage, the harness will have it. This means that, to prevent corona, the voltage between conductors minus the voltage drop across the insulation must be no greater than 325 volts where the air gap is 31 mils. Although the Paschen curve shows an increase in discharge onset voltage for smaller gaps, no advantage is available because the discharge can take a longer path that corresponds to the minimum onset voltage. Thus, the voltage must be no more than 325 volts for gaps less than 31 mils.

For the 230/400 nominal system voltage, the maximum peak potential between conductors is 896 volts peak for 0.11 second for abnormal conditions such as loss of control by the generator voltage regulator. Let us assume for the moment that corona can be allowed for this rare extreme transient condition. The maximum voltage for any normal transient is 738 volts peak. Let us assume that discharge onset must not occur at this voltage. Moreover, let us assume that transient induced voltages, such as those produced by switching off inductive loads, are suppressed to this peak value of 738 volts.

5.1.7.3 Determination of Insulation Thickness Required - Referring to Figure 4, at Section A-A let us now proceed to calculate the thickness of wire insulation required. Set the air gap equal to 31 mils. As a fair approximation, the region between conductors shown boxed by the dashed lines can be considered as two conductors separated by a layer of insulation on each, and the air gap of 31 mils. Insulation resistance will be neglected for the present, and will be discussed later. The dielectric constant of all insulation is greater than unity. It is about 2 for TFE Teflon, 3 for silicon, 3.0 for H-Film, and 3.3 for silicone rubber. Let us assume a value of two. At 738 volts peak between conductors and 325 volts across the gap, the drop across each layer of insulation must be half the difference, or 207 volts. Regard the air gap as a capacitor with plates 31 mils apart, and dielectric constant of one; and each layer

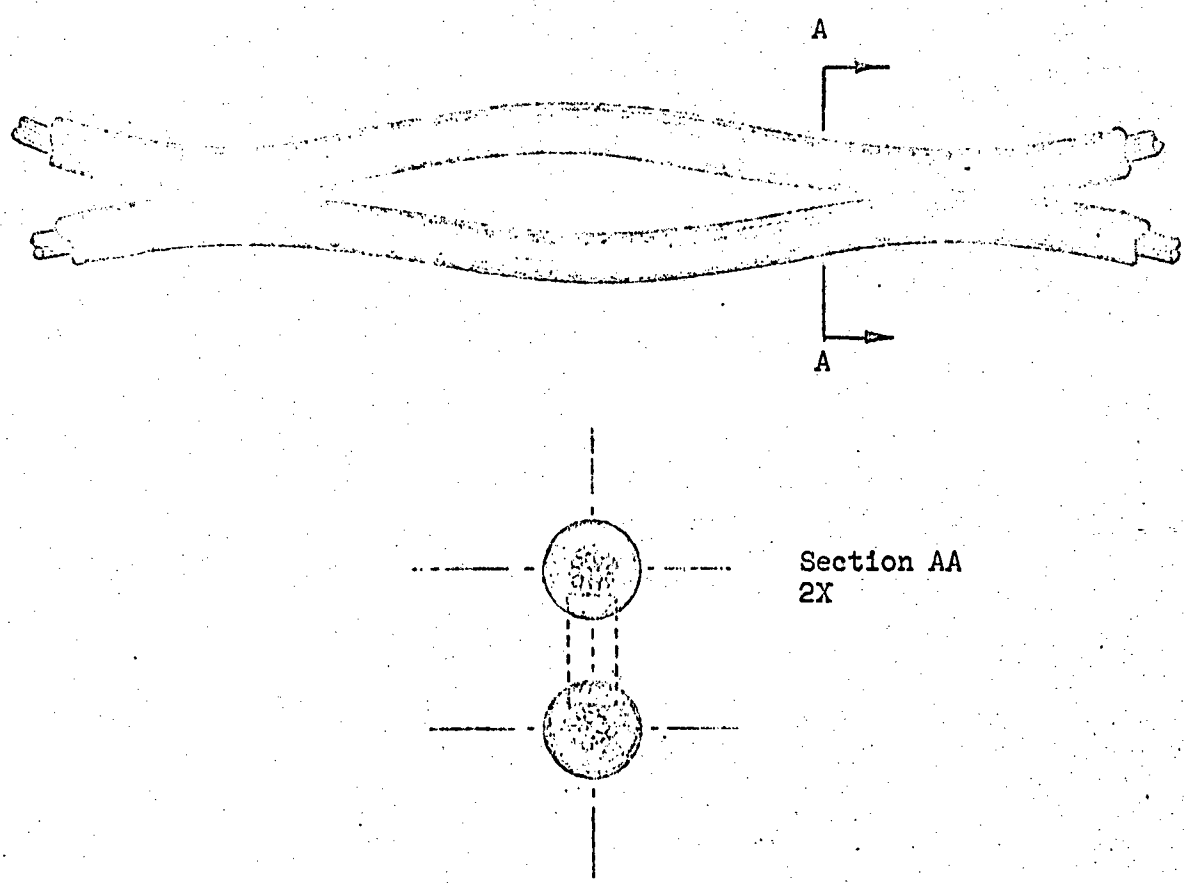

Figure 4 Conventional Insulated Wires

of insulation as a capacitor with plates separated by the thickness of insulation to be determined, and a dielectric constant of two. Since capacitance is inversely proportional to plate separation, and proportional to dielectric constant; and since the voltages across the capacitors will divide in inverse proportion to the capacitances, the required insulation thickness is:

$$T = \frac{1}{2}\left[\frac{V_c - V_g}{V_g}\right]\delta K \qquad (4)$$

where: T is the insulation thickness required in inches.
V_c is the peak voltage between conductors.
V_g is the peak voltage across the air gap.
δ is the width of the air gaps in inches.
K is the dielectric constant of the insulation.

This expression gives an insulation thickness required of 39.4 mils (0.0394 inch) for a dielectric constant of two. But the effective dielectric constant is about 2.5 for practical high temperature insulation systems, such as the insulation systems now being tested, which are made up of laminates of H-Film and TFE Teflon with and without a glass outer covering. This combination would require a minimum insulation thickness of 49.4 mils.

However, the worst-case insulation thickness required is not dictated by the breakdown voltage and gap at the minimum point of the Paschen curve, but by those for a point corresponding to a somewhat higher value of $p\delta$. For example, it is desired to determine the worst case $p\delta$ value and the corresponding required insulation thickness at 100,000 feet, 738 volts between conductors, and for a dielectric constant of 2.5. By evaluating Equation 4, with results as shown by Figure 5, the worst-case $p\delta$ value is 3.062 mmHg x cm (0.370 cm or 0.094 inch gap at 100,000 feet) and the corresponding insulation thickness required for prevention of sparkover is 0.1880 cm or 0.0742 inch.

Table I gives a fairly representative value of insulation thickness for various conductor sizes. By analyzing this, and remembering that 0.0742 inch

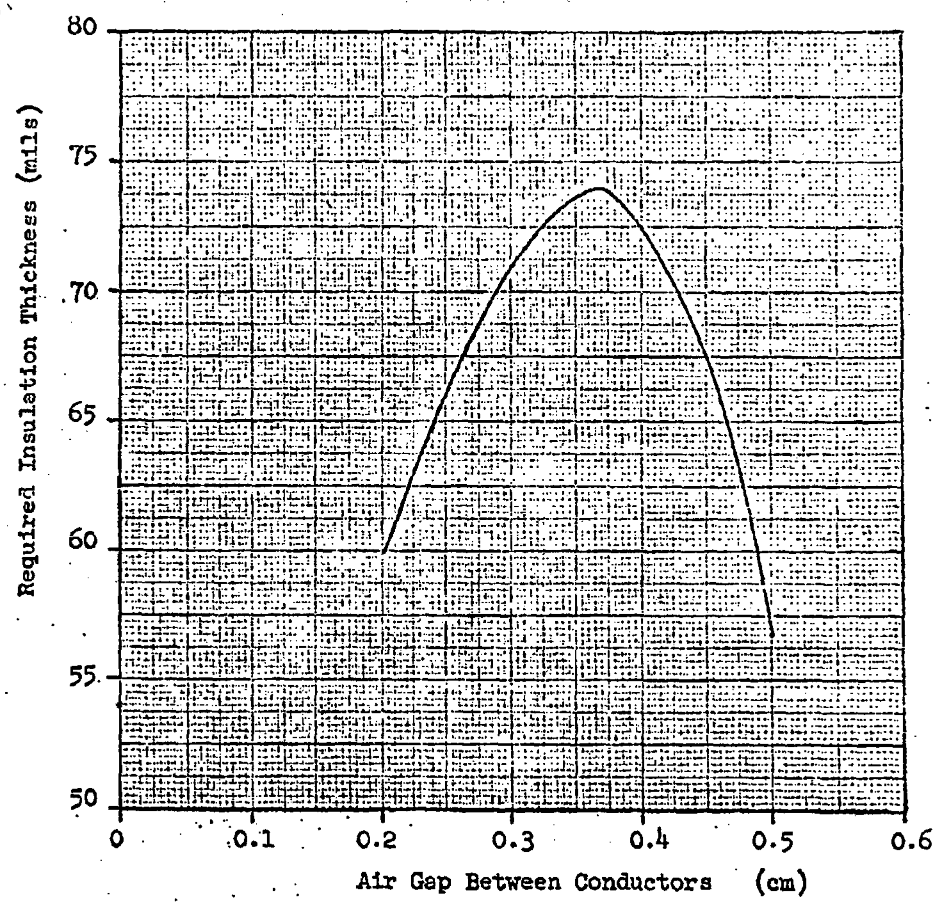

Assumed Peak Voltage = 738
Dielectric Constant = 2.5

Figure 5 Insulation required for various air gaps between conductors.

TABLE I

REPRESENTATIVE INSULATION THICKNESS FOR VARIOUS SIZED CONDUCTORS

SIZE NO.	TEFLON TFE HOOKUP WIRE TYPE EEW (Ref. 16)		INSULATION THICKNESS, IN.
	NOMINAL Cdr. DIA., IN.	NOMINAL O.D., IN.	
8	0.161	0.215	0.0270
10	0.113	0.149	0.0180
12	0.087	0.124	0.0185
14	0.069	0.105	0.0180
16	0.055	0.089	0.0170
18	0.048	0.079	0.0155
20	0.039	0.069	0.0150
20	0.038	0.068	0.0150
22	0.031	0.061	0.0150
22	0.030	0.060	0.0150
24	0.025	0.055	0.0150
24	0.024	0.054	0.0150

of insulation is required to eliminate onset at 738 volts peak and 100,000 feet, it is indicated that overall insulation thickness will be dictated by corona considerations.

Referring to Figure 4, it can be argued that where the two insulated wires touch an effective capacitor is shunting the gap, thereby reducing the gap voltage. This has been shown in tests wherein the onset voltage for twisted wires was somewhat higher than that for closely spaced wires. However, in conventional open wiring the wires can be separated slightly for several inches, so this shunting effect cannot be relied upon.

Note that corona can also occur in the unpressurized air spaces between the wire strands and the insulation.

5.1.7.4 Effect of Insulation Resistance or Surface Leakage - In the above discussion insulation resistance was neglected. Reference material (9) indicates that for some materials such as Teflon this factor is not negligible. Insulation resistance should be treated as a resistor in parallel with a capacitor representing the insulation, and would further increase the insulation thickness required or would render the insulation ineffective in supressing corona. This is shown in reference material (10) in which heated TFE Teflon-insulated wire, coiled and resting on a metal plate, produced corona onset at 220 volts rms which is slightly below the minimum peak value shown in Figure 1. This difference can probably be attributed to experimental error.

Surface leakage resistance between conductors, for insulation that is wet or has a conducting film, can enhance corona and sparkover. This situation may be treated as a voltage divider between the electrodes for determining the onset of corona at existing air gaps.

It may be argued that, as a lower limit, corona may be endurable for infrequent transient intervals at voltages somewhat above the maximum steady line-to-line value of 408 volts rms or 578 volts peak. However,

it is considered that design for no discharge onset below 738 volts peak is advisable. First a safety factor must be provided; also if corona onset is allowed, then the offset voltage value is much lower and difficult to predict accurately. Also insulation life has been affected to an extent difficult to evaluate quantitatively.

Referring to Figure 1, the air gap between bare terminals up to 100,000 feet (80,000 feet at 600 F) must be greater than 1.09 cm (0.428 inch) for 896 volts peak. To insure against sparkover, bare conducting surfaces should be avoided. In previous aircraft designs bare conductors have existed at terminal blocks, and between pins of connectors with hard inserts or imperfectly mated faces.

5.1.7.5 Determinations by Line-to-Neutral Voltages - Now consider the line-to-neutral voltages. Similar reasoning leads to design for $738/\sqrt{3} = 424$ volts peak. An insulated wire may lie against or near a grounded plate, and the worst-case air gaps must again be assumed. A method of calculation similar to that described above leads to a determination of the insulation thickness required. It is 20 mils, corresponding to a $p\delta$ of 0.095 mmHg x cm and a dielectric constant of 2.5. Note that this thickness is less than for line-to-line voltage (0.0742 inch) even though there is only one layer of insulation instead of two, and the applied voltage is reduced by less than two; actually by $\sqrt{3.0} = 1.73$. Nevertheless, corona considerations are still dictating insulation thickness. Note that the air gaps for bare conductors must be based on $896/\sqrt{3}$ or 515 volts peak, as damaging sparkover could otherwise result during an abnormal overvoltage transient. The corresponding gap is 0.133 inch and a safety factor must still be provided. For the line-to-line voltage the corresponding gap is 0.428 inch.

From the above analysis it can be seen that great advantages can accrue by adopting the design philosophy expressed in the conclusions. Whenever practicable areas should be avoided in which energized conductors, insulated or not, are adjacent to unpressurized air.

From the preceding discussion the marked effect is readily evaluated of changes in altitude and temperature. These alter the air density and affect greatly the required electrode spacings and insulation thicknesses required. At 80,000 feet and the applicable aerodynamic heating, the pressure is about 10 mmHg. At 80,000 feet and no heating it is about 20 mmHg, and the required spacings and insulation thicknesses are reduced by half. At 47,000 feet and no heating the pressure is about 100 mmHg, and the required spacings and insulation thickness are reduced by a factor of ten. It is therefore seen how pressurization markedly reduces the corona and sparkover problem. Also, it reduces the gains to be made by keeping the temperature low at the higher altitudes.

5.1.7.6 Precautions Still Required at Lower System Voltages - The peak voltage to be considered has a very marked effect on the spacings and insulation thicknesses required, especially at values near the minimum of the Paschen curve which is about 230 volts rms. In oversimplified theory no corona or sparkover can take place below this voltage regardless of spacings and insulation thickness. Practically, the same wiring methods that would eliminate the problem for the higher voltages, would still be advisable, as stated in the conclusions. For a lower system voltage such as 115/200 volts a-c or even 28 volts d-c, voltage transients between conductors from such operations as switching off inductive loads must be suppressed or spacings and insulation thicknesses provided so that corona or sparkover does not result.

5.1.7.7 Detail Design and Verification - For those areas in which energized wires, insulated or not, may be in contact with unpressurized air; guidelines for preliminary design have been presented above. For final design, numerous other factors must be considered as described in the following sections. Also, the final design configuration should be verified by conducting laboratory tests.

5.2 Supporting Information and Data

5.2.1 Electrode Configuration and Polarity.

The geometrical design of the electrodes, as well as the nature of their surfaces, can play an important part in facilitating electrical breakdown. Surface irregularities, such as sharp edges or points, produce a local concentration of the electric field which may well attain values at which true field emission of electrons might occur. Hence, to reduce the tendency to produce breakdown, all electrode surfaces should be smooth and as gently curved as possible.

It is also important to note that in most cases the corona inception voltage is lower when a point is negative. This occurs due to electrons which are starting at the most intense part of the field (i.e., at the electrode) where secondary emission processes are more efficient.

5.2.1.1 Breakdown Gradient as a Function of Electrode Shape - As discussed in 5.1.5.1, a conservative design practice is to avoid sharp radii and then design the spacings and insulation on the basis of the Paschen curve for point electrodes. If it is chosen instead to use the curve for parallel-plate electrodes (the upper curve in Figure 1) then some advantages can be gained, because this is the configuration for which electrical breakdown occurs at the lowest value of voltage gradient. This is explained in Sections 5.2.1.1.1 and 5.2.1.1.2. In such a case, the maximum point gradient for the actual electrodes can be combined with the Paschen curve for parallel plates (Figure 1, upper curve) to yield a safe design.

5.2.1.1.1 Secondary Products Loss - The parallel plate configuration provides the lowest secondary product loss factor of all the geometries. Photons are generated isotropically; i.e., they can be emitted in any direction. Hence with parallel plates, they either strike the cathode or anode. With other configurations, there is a non-zero probability of a strike on either plate.

Ions which are charged positive are attracted towards the cathode. In a parallel plate configuration, the ion has a certain probability of reaching the cathode. This probability is dictated by recombination rates of the gas. In other cases, the ion may miss the cathode or orbit around it. These added mechanisms reduce the number of ions available for cathode interaction for the non-parallel-plate case.

Excited atoms are isotropic in nature. In a parallel plate configuration these atoms have a certain probability of striking the cathode. This probability is dictated by the life of the excited state (metastable states have long life times) and the fact that the atom will strike either the cathode or anode. In other configurations, the atom can also escape the system, striking neither the cathode nor the anode.

5.2.1.1.2 Inelastic Collision Rate - The use of parallel plates, infinite in two directions, provides the greatest efficiency of secondary-electron generation. It will now be shown that parallel plates provide the greatest rate of occurrence of inelastic collisions. Figure 6 illustrates these arguments presented in the following two paragraphs. Suppose an electron is generated by an inelastic collision with a gas molecule. This electron has a probability of traveling a certain distance before striking a gas molecule. Such a probability is a function of the gas density, and size of the gas molecules, but not of electron velocity. Such a probability is also independent of field configuration.

There is a probability that the interaction between an electron and a gas molecule will be inelastic. The value of this probability is dependent on the energy of the electron; the lower the energy, the lower the probability.

Constraining our thinking to those cases where the voltage gradient of the parallel plate configuration is the same as the maximum gradient of the nonuniform field, Figure 6 implies that the energy of the electron interacting with the gas molecule is statistically lower than that of the parallel plate. This implies a lower probability of inelastic collisions.

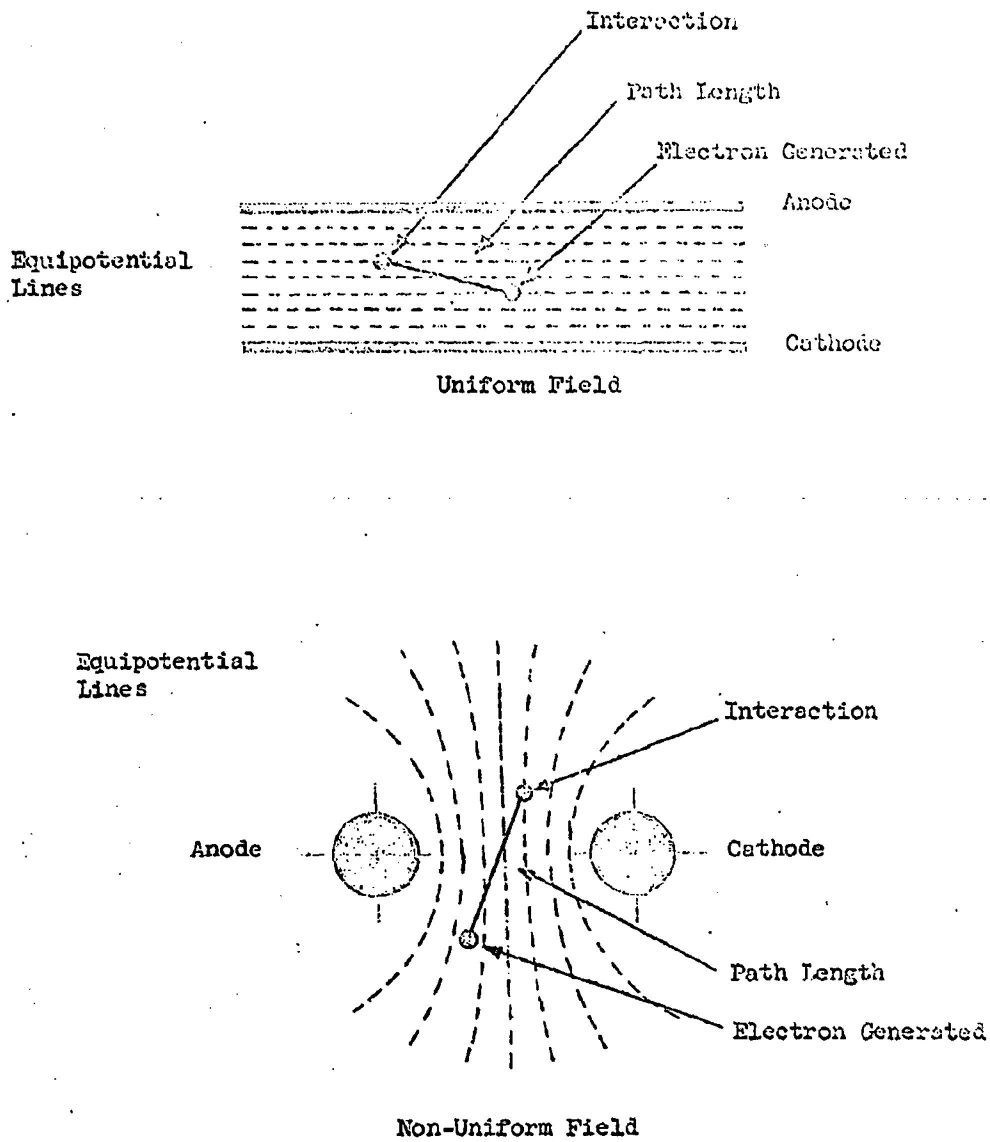

Figure 6 Comparison of Parallel Plate Configuration and Non-Uniform Fields.

In rating various configurations of conducting surfaces for the avoidance of electrical breakdown, it is sufficient to require that the maximum voltage gradient shall be less than that specified by Paschen's Law curve for parallel plates as shown in Figure 1.

5.3 Transient Conditions

The time of voltage application is believed to play an important part in determining the pre-breakdown currents or the breakdown threshold. When a field sufficiently large to cause breakdown is applied to a system of electrodes, there are two reasons why sparkover does not immediately occur: (1) time is required for one or more initial electrons to appear in a favorable position in the gap to lead to the necessary avalanches. This is called the statistical time lag, (2) the development of these avalanches and buildup of current to a value corresponding to breakdown requires time because of the finite mobilities of the particles. This is known as the formative time lag. Thus, there is a time delay before breakdown which is the sum of these two periods.

In the case of air, the statistical time lags are in the order of microseconds and the formative time lags are even smaller. This occurrence of breakdown during any particular application of voltage will therefore depend on the time of voltage application and would occur with some probability rather than certainty.

The statistical time lag is analyzed by making a large number of tests of breakdown at a given voltage with an essentially square front pulse and recording the time to breakdown. The value of time corresponding to $n/N = 1$ is the formative time lag. This relation is expressed mathematically as:

$$\ln (n/N) = -\lambda t \quad (5)$$

where n is the number of tests and N is the total number of breakdowns with a time lag of τ or greater. $1/\lambda$ is called the mean statistical time lag. It is a measure of the mean time between occurrences of breakdown initiating electrons in the gap.

The mean statistical time lag decreases markedly with the ultraviolet irradiation of the cathode which increases the supply of electrons and also decreases with increasing voltage. With an unirradiated gap in which cosmic rays and radioactive impurities are the sole source of electrons, the time lag will again be largely statistical. In a gap purposely irradiated, the statistical time lag may be sufficiently reduced so that the principal contribution to the total lag comes from the formative part. Therefore the two time lags are separated and measured experimentally in this manner. These time lags are of considerable practical as well as theoretical interest, since if the duration of an applied voltage pulse approaches the time lag, an appreciable increase in breakdown voltage may be observed.

For the practical purposes of this investigation these time lags, if ignored, can lead to discharge onset voltage determinations that are high by one or two percent (Ref. 11).

5.4 Influence of Magnetic Fields

As electrons travel between the cathode and anode their free paths between collisions are bent by magnetic fields in accordance with the relation:

$$Heu = mv^2/r \tag{6}$$

where
- H = magnetic field intensity
- e = electron charge
- u = path length between collisions
- m = mass of electron
- v = electron velocity
- r = path radius

Now, consider the case where the magnetic and electric fields exist parallel to each other. For high gas densities, the mean free path of the electrons is smaller than the interelectrode distance and gas collisions then become significant. In accordance with Equation 6 the lateral diffusion is thus reduced and the maintenance of the discharge is faciliated. For lower densities when the mean free path is of the order of, or greater than, the electrode distance; the electrons are free in their passage between the cathode and anode and their free paths become curved in such a manner to further facilitate discharge.

Next consider the case of a transverse magnetic field parallel to the electrode surface and thus at right angles to the electric field. Due to the interaction of this magnetic field, it is necessary to consider the distribution of free paths about a mean value and also electron reflection at the cathode. Their effect on the maintainance of discharge depends on the gas density and on the parameter $p\delta$ (pressure x electrode spacing); thus the location on the Paschen curve. For example, if the magnitude of $p\delta$ is greater than that corresponding to the Paschen minimum, then a transverse magnetic field effectively increases $p\delta$ so that a higher breakdown potential is required. On the other hand if $p\delta$ in an evacuated vessel is less than that corresponding to the Paschen minimum, then the transverse magnetic field which in effect increases $p\delta$, reduces the breakdown potential.

Thus the influence of any magnetic field on breakdown potential, as well as that of electrode geometry, depends on a value for the parameter $p\delta$.

For the purposes of design, it is considered that magnetic fields can be ignored, since significant fields will not generally exist except from wires carrying current. The latter fields will be transverse to provide added safety against discharge.

As for the low values of pδ, no safety is lost, as the effect will not alter the minimum point of the Paschen curve. Moreover, no advantage is available from the higher onset voltage at the low pδ end of the curve. This is because for practical configurations the discharge can take a path of greater than the minimum length that will correspond with the minimum point of the Paschen curve.

5.5 Dielectric Materials As Insulators

5.5.1 Definitions and Explanations

5.5.1.1 Dielectric Strength - Dielectric strength is that voltage which an insulating material can withstand before breakdown occurs and is usually expressed as a voltage gradient such as volts per mil.

5.5.1.2 Dielectric Loss - Dielectric loss is the time rate at which electric energy is transformed into heat in a dielectric when it is subjected to a changing electric field. A low loss is a requirement for high quality insulation.

5.5.1.3 Dielectric Absorption - Dielectric absorption is that property of an imperfect dielectric whereby there is an accumulation of electric charges within the body of the material when it is placed in an electric field. A low dielectric absorption is necessary to prevent low values of breakdown voltage.

5.5.1.4 Dielectric Power Factor - Dielectric power factor is a measure of the relative dielectric loss in the insulation when the system acts as a capacitor. A low power factor is considered a criterion of high-quality insulation.

5.5.1.5 Surface Resistivity - Surface resistivity of a material is the resistance between two opposite sides of a unit square of its surface. A high surface resistivity is desired to prevent low values of voltage breakdown.

5.5.1.6 Surface Leakage - Surface leakage is the passage of current over the boundary surfaces of an insulator as distinguished from passage through its volume. It is a very undesirable effect and is usually attributed to conduction within surface films.

5.5.2 Effect of Electrical Discharge Near Dielectrics

5.5.2.1 Factors Affecting Breakdown - The dielectric breakdown strength of a material depends on a number of factors including atmospheric conditions, voids, and dielectric composition. It is also dependent upon the rate and duration of dielectric stress as covered in Section 5.3 on transients.

5.5.2.1.1 Atmospheric conditions

5.5.2.1.1.1 Moisture contamination

The dielectric breakdown strength of an insulation is seriously reduced by moisture contamination.

In a dry homogeneous insulation, ions are held together by strong attractive forces. After water absorption interfacial polarization exists which decreases this attractive force according to Coulomb's Law. This allows the ions to dissociate and migrate in the direction of the electric field. As a result there is a disadvantageous increase in capacitance and dielectric power factor together with a serious reduction in surface resistivity.

The rate of moisture absorption and the degree of retention of moisture depend upon the porosity of the material, the relative humidity and temperature, and upon the frequency of the applied voltage.

Even with non-porous insulations surface films of moisture or dew may form as a result of changes in atmospheric conditions. This thin film of water may render the surface highly conductive which constitutes surface leakage and possibly voltage breakdown. Whether or not a complete film is formed depends upon the ease with which the water wets the insulation surface.

Even microscopic roughness aids the formation of moisture films. Dirt, dust or other contaminants on an insulating surface may also greatly increase the tendency for the formation of conductive films which absorb moisture. Also the possibility must be considered of the presence of salt, oil, smog, solvents, cleaning fluids, etc.

5.5.2.1.1.2 Temperature and density

A change in temperature influences the corona starting voltage through its effect on the air density, dielectric constant of the solid, and the thermionic emission of the cathode.

It has been found empirically that the density effect can be taken into account by multiplying the corona starting voltage at room temperature (20 C) and atmospheric pressure by 293/T where T is the absolute temperature in K which is equal to C + 273 (Ref. 12).

The effect of temperature on the dielectric constant is dependent upon the type of material used. For example: The dielectric constant of Teflon resins and H-Film decreases, whereas, that of silicones increases with temperature.

When a conducting surface is raised to a sufficiently high temperature, an appreciable number of electrons will have the kinetic energy required to escape through the surface of the material. This results in thermionic emission of electrons. Heated materials, especially titanium, are known to liberate large amounts of electrons which enhance electrical breakdown. The extent of corona on heated titanium surfaces is discussed in Lockheed Report 18481 (Ref. 3).

Over the range from atmospheric density to moderate vacuums, a decrease in density will reduce corona starting levels and will increase the effective gap spacing for minimum starting voltage. This effect is accounted for by Paschen's Law curve which expresses onset voltage as a function of gas density and spacing.

Consider the case of a void trapped within an insulation at the time of manufacture. It is desired to determine what effect SST altitudes and temperatures will have on this void. At manufacture the pressure within the void is say 760 mmHg (14.7 psi) and the temperature as a worst case is say 20 C (68 F). At the SST altitude of 80,000 feet and temperature of 600 F (310 C), pressure within the void is calculated from the constant volumn gas law, where p is the pressure in mmHg and T in degrees absolute.

$$\frac{P_1}{T_1} = \frac{P_2}{T_2} \qquad (7)$$

$$\frac{(760)\text{mmHg}}{(20\text{ C} + 273)} = \frac{(P_2 - 760 + 10)\text{mmHg}}{(310\text{ C} + 273)}$$

$$P_2 = 2270 \text{ mmHg or } 43.5 \text{ psi}$$

This means that, due to a void, the insulating material has to withstand an internal pressure of 43.5 psi to maintain its integrity.

5.5.2.1.2 Dielectric Composition - The dielectric breakdown strength and corona resistance of an insulating material is dependent on non-excessive conduction through the insulation.

With some exceptions (notably sulfur and diamond) solid inorganic insulating materials are ionic crystals, or glasses that have amorphous structures. In such structures all atoms are ionized but bound, with only a few exhibiting random distribution. The smaller positive ions (hydrogen, sodium, potassium, etc.) move more easily through the material and when present contribute most to the ionic conductivity.

In contrast, pure organic materials contain relatively few ions; the atoms of organic molecules being bonded by non-coulomb forces, wherein electrons are mutually shared, rather than being completely transferred from one atom to another. The ions that are present in organic insulating materials, are

usually products of oxidation or other degradations of the insulation. Therefore, the ionic conductivity of organic electrical insulation is subject to wide fluctuations, depending on the purity or history of the material.

Dipole molecules also conduct for short periods of time by rotating in the direction of the field. Therefore dipoles contribute to d-c conduction only for a short period after voltage is applied and to a-c conduction only at higher frequencies.

Whenever conducting ions or dipoles are able to move rapidly enough to go to the limit of their movement, within a small fraction of a cycle, they produce a current that is maximum at zero voltage. This is characteristic of a capacitance which is proportional to the dielectric constant. Materials that have a large number of dipolar molecules or parts of molecules have an undesirable high dielectric constant, high conductivity, and a high power factor.

5.5.2.2 Corona Aging of Materials

5.5.2.1 Surface Corona - Surface corona is not harmful to many forms of insulation, but there are serious secondary effects due to the production of powerful oxidizing agents in an intense electrical field. Ozone is produced, accelerating the oxidation of organic materials, and nitrogen oxide compounds result from the ionization of the air. These combine with water to form nitric acids which attack not only organic compounds, but also corrode metal. Cellulose and organic fluorocarbon resins such as Teflon are rapidly oxidized in corona fields as they are embrittled, weakened mechanically, and then destroyed.

Corona degradation of Teflon is a direct result of bombardment by high energy gaseous ions accelerated by the electric field (Ref. 13). These ions bombard the walls of the cavity, breaking down the insulation and enlarging the voids. This process continues until the insulation is penetrated causing dielectric failure. A similar result is observed when an organic material is bombarded with high-energy radiation.

Mica and glass are not affected either by corona or by oxidizing agents produced by it because of their inorganic structure. Silicone resins are more resistant to corona than their organic counterparts. Organic synthetic rubbers and natural rubbers are both susceptible to corona attack but silicone rubbers are highly resistant.

One manufacturer (Ref. 14) has claimed to have developed a new line of high voltage wire and cable which uses CR (corona resistant) Teflon to overcome the problems caused by corona. This new insulation is specifically designed to prevent or retard corona penetration. It contains a small amount of additive that is dispersed as tiny particles about one micron in diameter. Under the ion impacts of corona, the dispersed material forms a liquid which covers the surface being bombarded. This protective film in CR Teflon prevents or slows down the growth of the cavity. The protection is essentially complete if the impact energy of the ions is below the level required to penetrate the liquid film and strike the solid dielectric beneath. Even at high energy impact levels, the liquid film absorbs much of the impact and greatly reduces the penetration rate through the insulation. Thus, the major effect of the corona resisting additive is at intermediate voltage stresses where the liquid film is essentially impervious to ion impacts.

The manufacturers evaluation of test data and actual experience under use conditions has established the voltage ratings, as shown in Table II, for high voltage cable with CR insulation of varying thickness. The constructions in this table have been designed for a minimum life of 10,000 hours. Longer or shorter life can be accomplished by a logarithmic function of the insulation thickness. For example, doubling the thickness will increase the minimum life at least tenfold; halving the thickness will reduce the life to about one tenth - or 1000 hours.

CR Teflon insulations are rated from -60 C to 300 C, although the corona initiation voltage is somewhat lower at high temperature.

TABLE II

VOLTAGE RATINGS OF VARIOUS INSULATION THICKNESSES FOR CORONA RESISTANT TEFLON

DESIGN INFORMATION FOR HIGH-VOLTAGE CR CONSTRUCTION MINIMUM LIFE EXPECTANCY 10,000 HOURS				
INSULATION THICKNESS (INCHES)	AC VOLTAGE RATINGS		DC VOLTAGE RATINGS	
	SEA LEVEL	80,000 FT.	SEA LEVEL	80,000 FT.
.025	3,750	2,500	12,500	8,500
.030	4,500	3,000	15,000	10,000
.035	5,250	3,500	17,500	11,500
.040	6,000	4,000	20,000	13,500
.050	7,500	4,500	25,000	15,000
.065	10,000	6,000	32,500	19,500
.080	12,000	7,500	40,000	24,000
.100	15,000	10,000	50,000	33,500

5.5.2.2.2 Corona Breakdown Processes in Insulation - Dielectric breakdown usually results from an electron avalanche in the dielectric. In a few cases breakdown results from excessive heating of a highly conductive insulation by the electric field until it decomposes to conducting carbon (in the case of organic insulation), or becomes a molten electrolyte (in the case of ceramics).

Electron avalanches are now believed to occur not only in gases but also in solids and liquids. Once breakdown begins within a solit at an edge or point it continues through the material. At an instant determined by cumulative electrical, chemical, and mechanical effects, a breakdown channel, often microscopic, penetrates the eroded surface.

The propagation of a breakdown is likely to be a random branching process known as "treeing". This slow erosion to tree propagation is believed to begin when a pit is eroded through the wall of a void, it is thought to act as a sharp pointed conductor. Because of stress concentration, the gradient at the tip of such a pit can exceed the intrinsic strength of the insulator even thougn the average field between conductors is within the limits of the dielectric. Under these conditions, the dielectric ahead of the pit breaks down thereby extending the pit as a fine channel. This effect is attributed to the formation of space charge around a point conductor. With sinusoidal applied voltages, the space charge evidently stays in phase with the polarity of the point so that its effect is always to reduce the field. However, if sudden changes in potential occur, the space charge cannot form or if formed is unable to immediately adjust to the new point voltage. In this case, high transient stresses can momentarily exist at the end of the needle or eroded pit which then continue the process of degradation. This dependence of the stress on the rate of voltage change can explain why transients have been observed to start breakdown.

Trees in some cases appear to be non-conductive to DC voltages but become increasingly conductive with higher frequency AC voltages. In high frequency applications the AC conductivity of insulation also leads to a large amount of dielectric heating, and a low power factor is a necessity to prevent the destruction of the insulation.

Often if mechanical forces are present electrical failure may occur as a result of the degradation of mechanical properties of the materials by the discharges. For example, in many polymers, cross linking reactions may cause embrittlement, with ultimate failure due to cracking. Materials under mechanical strain may undergo "stress-cracking" or "ozone cutting" owing to scission of polymer chains by the discharges or their products.

Corona degradation of insulation for the SST will be of no significant problem, since design criteria will require corona onset not to occur. If corona does occur, it will persist only under a rare transient condition.

5.5.9 Dielectric Effect on Corona and Sparkover

Once we stress the air with intense flux fields we must then explore the quantity of ions in absolute numbers between the electrodes. The entire path between the electrodes must be overstressed to permit sparkover or flashover whereas corona exists when part of the path is overstressed. Current can pass uninterrrupted as sparkover; but, the passage of this extreme current is usually prevented by the inclusion of a dielectric. In this case only corona will result. When there is no solid insulation separating two electrodes dielectric breakdown and arc-over generally closely follow the formation of corona. Corona will also occur at the interface between a solid and a gaseous insulation. Here breakdown does not immediately follow unless the total voltage exceeds the dielectric strength of the solid insulation alone.

The original voltage distribution is determined by the relative spacing and the dielectric constants of the respective materials. An increasing dielectric constant contributes to capacitance by effectively moving the

"plates" closer together. However, when corona is formed, the voltage across the gas space collapses thereby imposing the full voltage across the solid insulation.

6.0 LABORATORY TESTS

6.1 Test Procedure and Corona Test Circuit

The method selected for electrical discharge detection measures the voltage produced across a resistor by the discharge as shown in Figure 7. The voltage output is then fed through a high-pass filter and a wide-band amplifier to an oscilloscope. This circuit is simple to operate, provides consistant results, has adequate sensitivity, and is insensitive to outside interference. The overall corona detection test setup is shown in Figure 8.

Data was taken by pumping down the chamber to an equivalent SST altitude and temperature by accounting for the temperature as only a change in density. (80,000 feet at 600 F is approximately equal to 100,000 feet at room temperature or 68 F.) The system voltage was then increased at a rate of approximately 100 volts per minute until onset occurred, and then decreased to determine the extinction potential. This process was repeated several times to obtain a set of readings for the purpose of reliability. The system was purged several times during each test to eliminate the effects of ozone and other impurities.

The electrical discharge onset voltage was determined by applying a voltage to the test specimens within a frequency range of 60 cps to 1000 cps. No significant difference in onset voltage resulted from this change in frequency.

It is again pointed out that most of the testing done was to verify data found in several references which appeared to be related to actual SST environmental conditions. For this reason, results were taken only at 100,000 feet (80,000 feet at 600 F) and represent the most severe cases for corona considerations.

Determinations were made of corona and arc-over for specimens of insulated wire, and also for several electrode shapes.

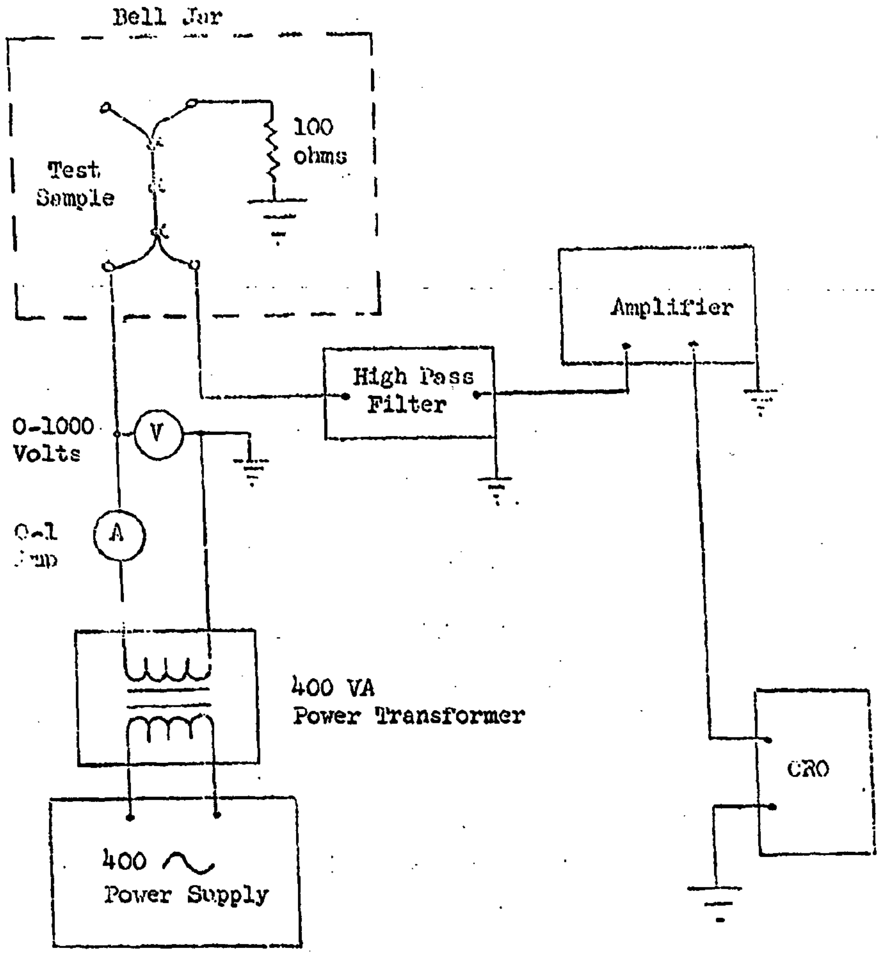

Figure 7   Corona Test Circuit

Figure 9 shows the test setup for various spacings of needle-point configurations. Several types ranging from rounded points to very sharp points were tested to determine which yielded the least onset voltage at a given spacing and altitude (p δ).

The use of a three-phase, 4 wire "Y", a-c power generating system dictates the possibility of corona onset between line-to-line and line-to-neutral wiring configurations.

Figure 10 shows the test setup for parallel wires which represent various line-to-line voltages and spacings. Precautions were taken to ensure that the wires remained parallel for a given air gap so that accurate test results could be obtained. The air gap between the wires was kept uniform at a given spacing ±0.001 inch. Tension was maintained in the conductor by use of the "clamping block" shown in the figure.

Figure 11 shows the test setup for a wire and a ground plane which represents various line-to-neutral voltages and spacings. Again precautions were taken and accuracy was maintained to ensure good test results.

6.2 Analysis of Comparable Data From Laboratory Tests and References

The purpose of the laboratory tests was to check the consistency of the reference data and to correlate this data with Equation 4, Page 16, to determine whether any limitations exist on its application. A major portion of the reference data was found to be inconsistent, which can probably be attributed to error in laboratory procedure. Reference material (Ref. 28) on #18 conductor agreed quite well with experimental data obtained in the Lockheed Electrical Systems Laboratory and for this reason it is used as an example in this section. Also, reference material (Ref. 28) on other sizes of bare conductors was not greatly different than that for #18. This is shown by considering (for a given air gap between a large and a small conductor) that the data points for the large conductor will approach the curve for parallel plates and data points for the small conductor will approach the curve for points.

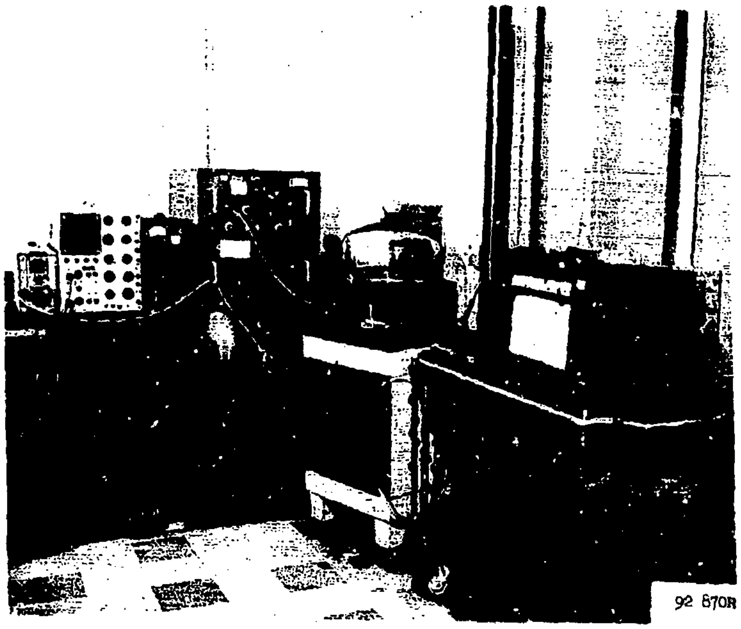

Fig. 8 - Test setup for corona detection.

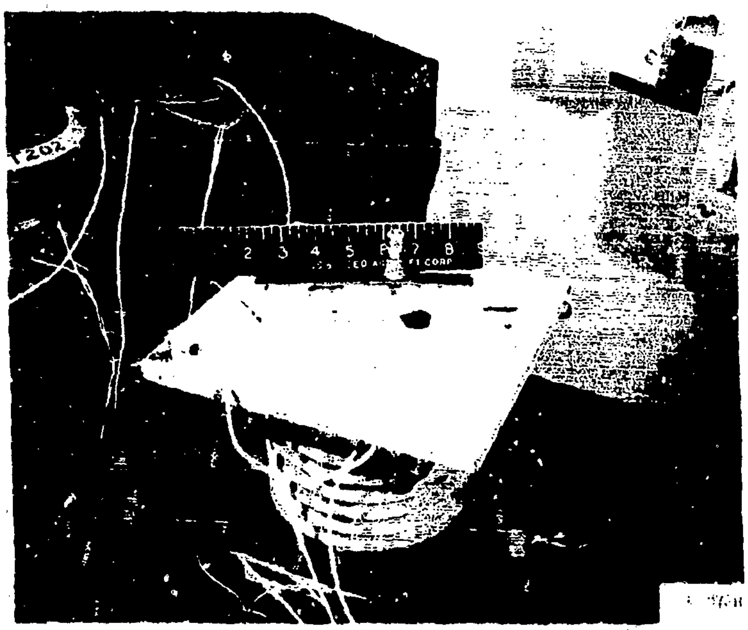

Fig. 9 - Test setup for various spacings of needle-g[illegible] configurations. (Note points between numbers 5 and 6).

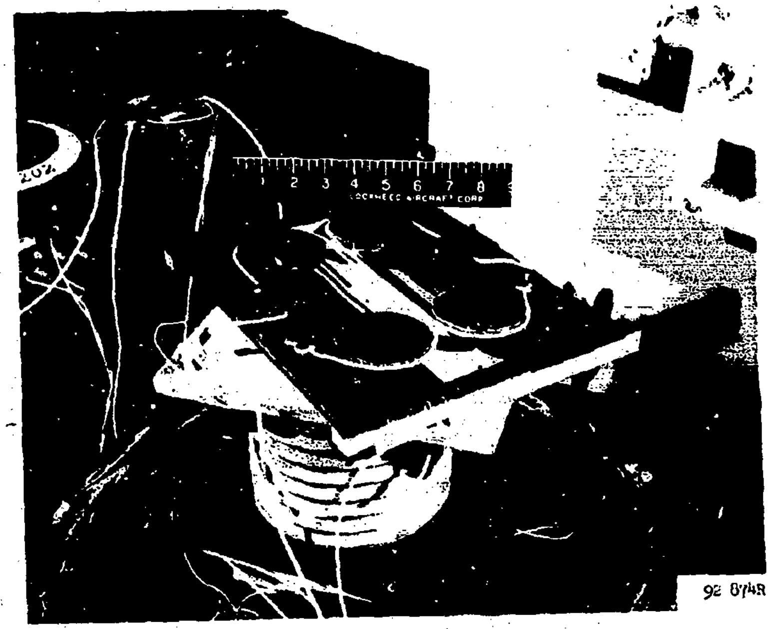

Fig. 10 - Test setup for parallel wires at various line-to-line voltages and spacings.

Fig. 11 - Test setup for a wire and ground plane at various line-to-neutral voltages and spacings. (Note conductor reflection on metal plate).

Figure 12a represents the case of two parallel, non-insulated stranded wires. Test results were obtained from the test setup shown in Figure 10 except that the insulated wires were replaced with bare, stranded conductors. Test data is shown on Figure 13 where it is compared with the modified Paschen curve of Figure 1 and to comparable data from Ref. 28. Data points occur between the curve for parallel plates and the curve for points, as expected, due to the shape of the configuration. Although not shown on Figure 13, similar tests were run for #18 solid conductors. Test results indicated that corona onset is slightly lower for stranded, bare conductors due to the smaller radii of the strands.

Figure 12b represents the case of an insulated conductor next to a ground plane, as could occur with line-to-neutral voltages where a conductor is near a grounded panel. Test results were obtained from the setup shown in Figure 11. On Figure 14 these results are compared to the modified Paschen curve of Figure 1; to comparable data from Ref. 28; and to onset voltages calculated from Equation 4. Note that Equation 4 is for parallel insulated conductors and must be modified by removing the constant 1/2 to account for only one insulation thickness.

$$T = \left[\frac{V_c - V_g}{V_g} \right] \delta K \qquad \text{Eq. 4.1}$$

Given the insulated wire next to a ground plane, as in Figure 12b, it is desired to determine the onset of corona for a given spacing and altitude. Consider, as an example, a spacing of 0.1155 inch (0.294 cm) and an altitude of 100,000 feet (8.29 mmHg.). The breakdown voltage of the air-gap is determined from the Paschen curve of Figure 1. For a pδ of 2.1 mmHg x cm (8.29 mmHg x 0.294 cm), V_c is determined to be 520 volts peak from the curve for parallel plates and 480 volts from the curve for points.

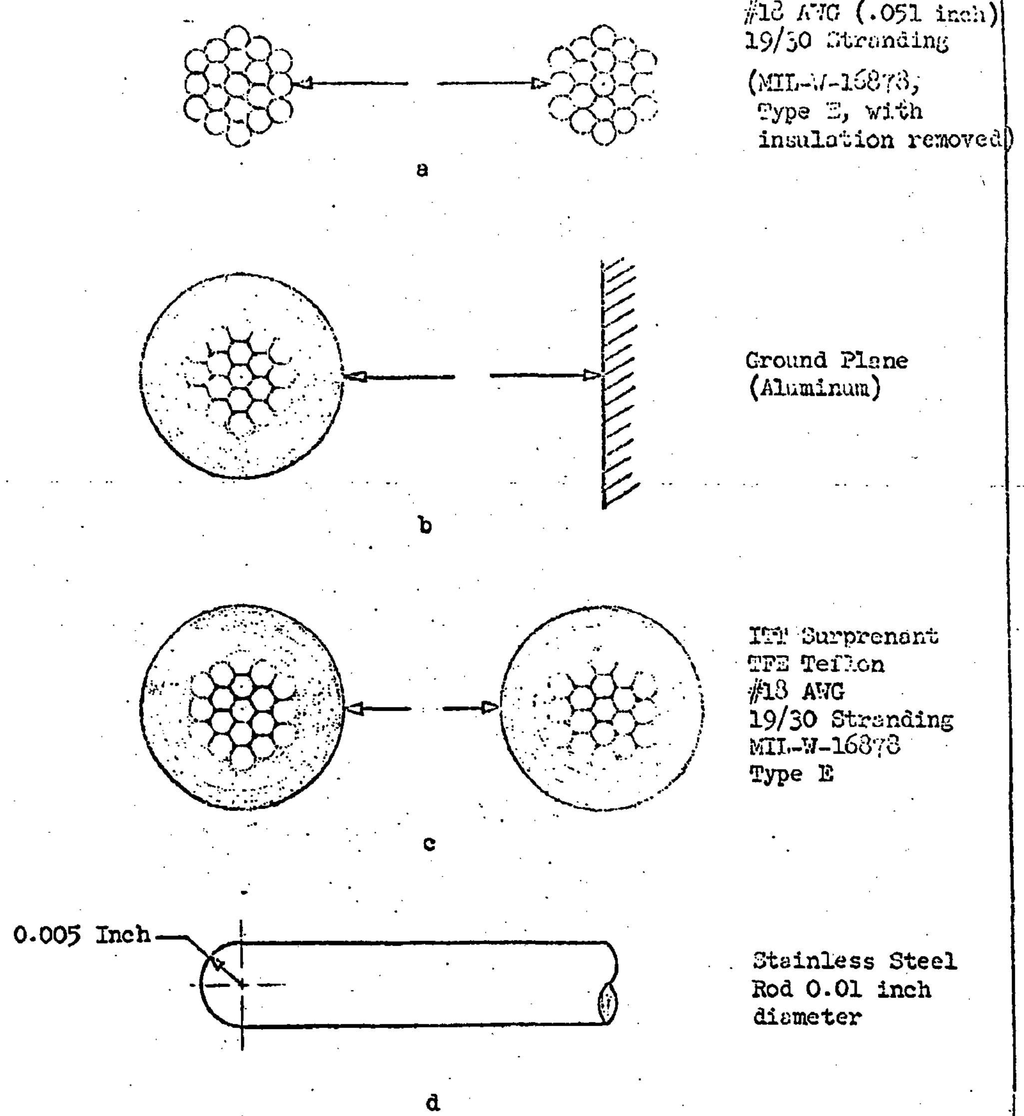

a. Cross section of test sample, parallel, bare, stranded conductors.
b. Cross section of test sample, parallel, insulated, stranded conductor and a ground plane.
c. Cross section of test sample, parallel, insulated, stranded conductors.
d. Cross section of test sample needle-points.

Figure 12 Electrode Configurations Tested

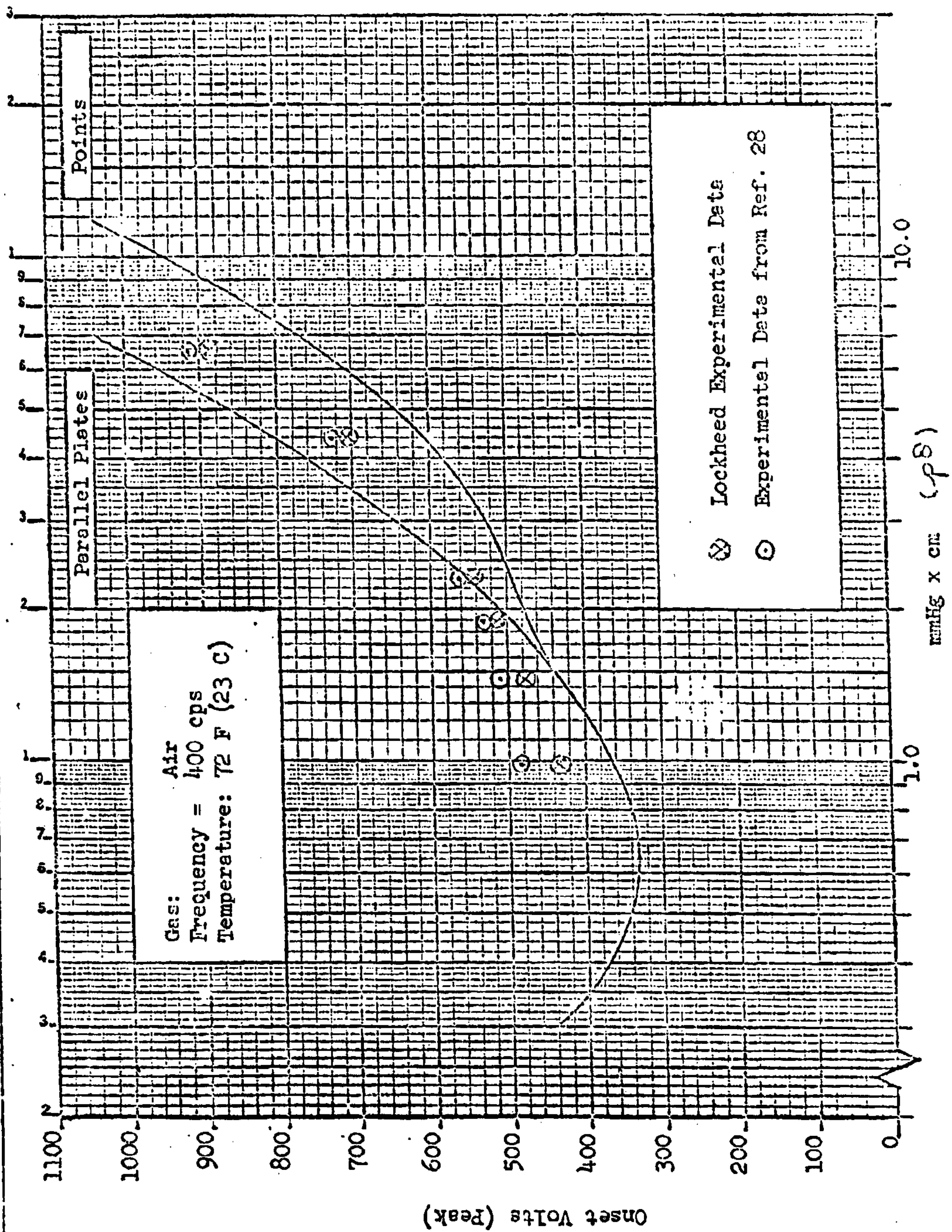

Figure 13 Comparison of Paschen curve of Figure 1 with behavior of #18 bare, stranded, parallel conductors.

Considering the conservative value for points and solving Equation 4a for the corona onset voltage V_c :

$$V_c = V_g \left[\frac{T}{K\delta} + 1 \right] \qquad \text{Eq. 4.1.1}$$

$$= 460 \left(\frac{0.0105}{2.1 \times 0.1155} + 1 \right)$$

$$V_c = 500.8 \text{ VOLTS PEAK}$$

Similarly, considering the curve for parallel plates:

$$= 520 \left(\frac{0.0105}{2.1 \times 0.1155} + 1 \right)$$

$$V_c = 542.5 \text{ VOLTS PEAK}$$

Both of these calculated values appear on Figure 14 for a $p\delta$ of 2.1 mmHg x cm. A family of curves may be plotted in a similar manner for different spacings and altitudes. It is interesting to note that the configuration of a closely spaced conductor and a ground plane more closely represents parallel plates than points. Therefore, it seems reasonable that the actual corona onset voltage will closely approximate the curve for parallel plates as calculated above. This is shown to be true by analyzing Figure 14.

It should be noted that wiring has to be terminated by connectors or terminals and the possibility of sharp points enters the picture. Therefore, for design criteria it is desirable for calculations to be based on the curve for points.

Figure 12c represents the case of two parallel insulated wires. Test results were obtained from the setup shown in Figure 10. On Figure 15 these results are compared to the modified Paschen curve of Figure 1; to comparable data from Ref. 28 and to onset voltages calculated from Equation 4. Due to the presence of two insulation thicknesses between conductors the constant (1/2) must be considered as discussed above. A family of curves may be plotted in a similar manner as discussed previously.

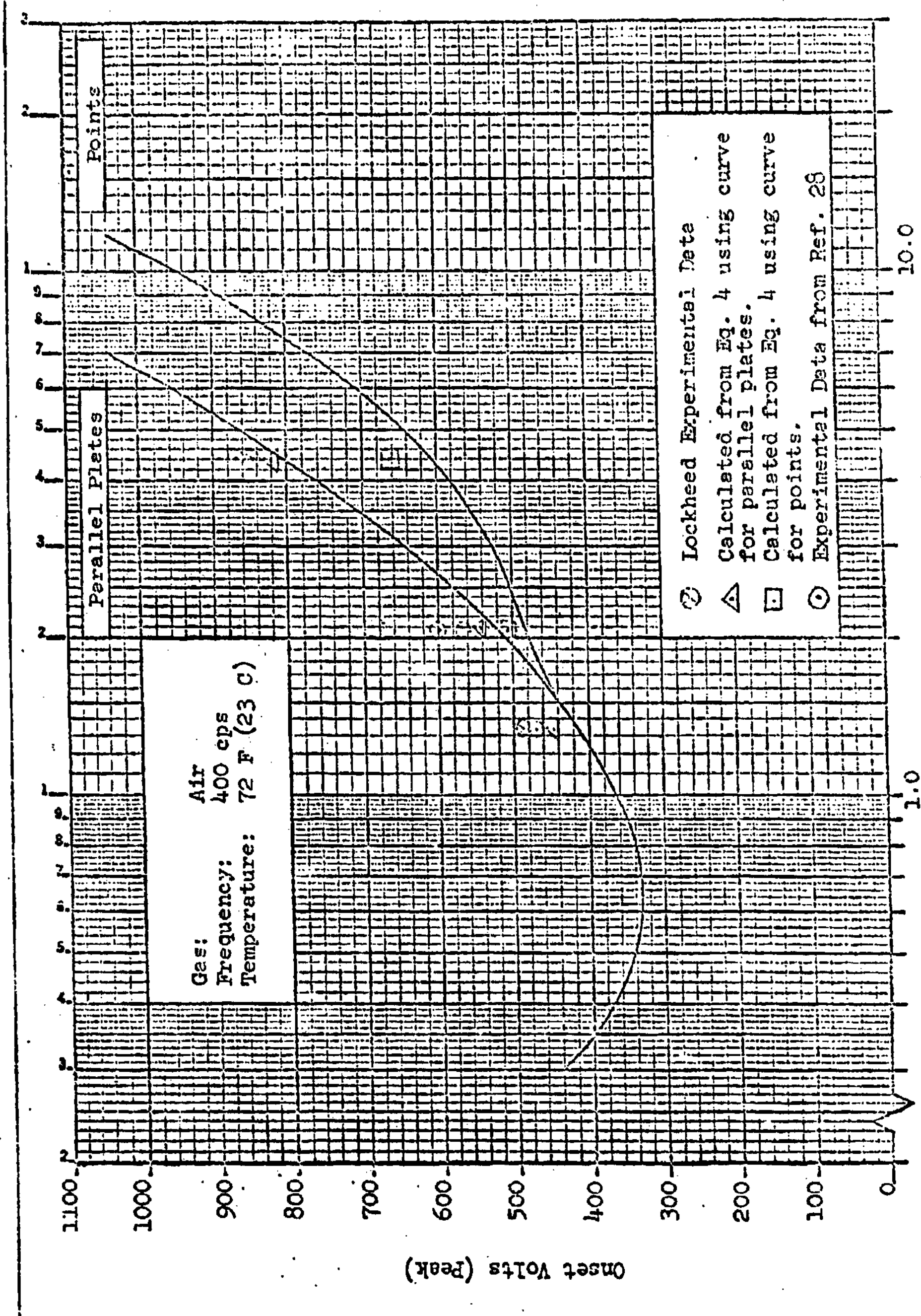

Figure 14. Comparison of Paschen curve of Figure 1 with behavior of a #18 stranded, insulated conductor next to a ground plane.

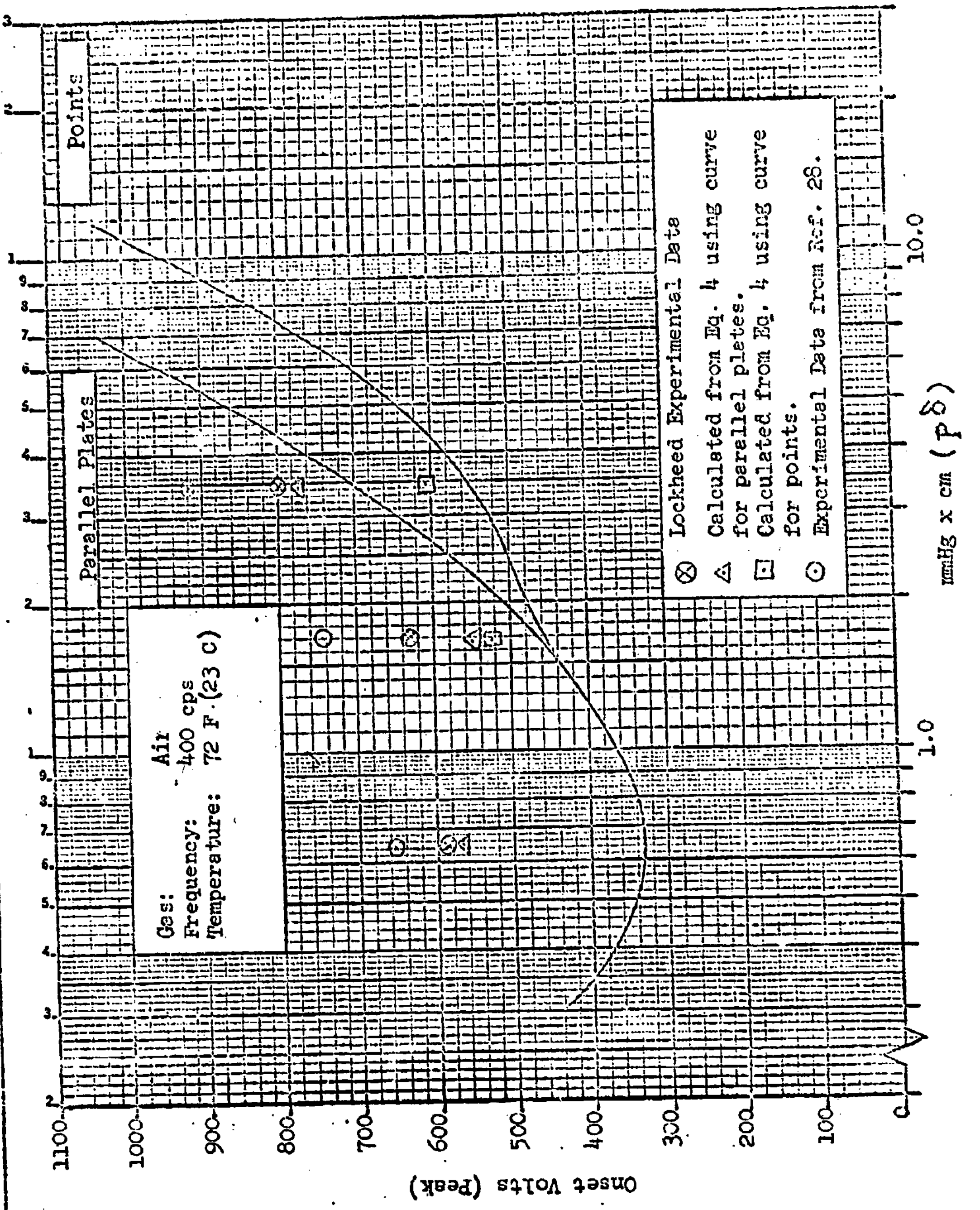

Figure 15 Comparison of Paschen curve of Figure 1 with behavior of #18 stranded, insulated, parallel conductors.

Figure 12d represents one case of a sharp point which could occur within a connector. Figure 16 compares laboratory data for 0.01 inch diameter needle points to the Paschen curve of Figure 1. Reference material (Ref. 15 and Ref. 28) indicates that very sharp pointed isolated electrodes will define the modified Paschen curve for points as also shown on Figure 16.

The tests also indicated that sharp points near large conductors do not represent as undesirable a condition as would be indicated by tests on isolated needle points.

Although insulation on wires in general prevents arc-over at lower voltages, the appearance of corona is not prevented and sometimes occurs at lower voltages than without insulation. This corona discharge, although not immediately damaging, does result in eventual damage to the insulation. It was noted that the same size of bare wire and the same spacing, spark-over occurred without any preceding corona discharge at low altitudes but corona occurred before sparkover at high altitudes. It is important, also, to note that corona, once started, can be sustained at voltages well below the onset voltage. Insulated conductors were found to have offset voltages as much as 50 volts below their onset values; while non-insulated parallel plates sometimes have offset voltages corresponding to a value around the minimum of the Paschen curve. Offset voltages were found to defy analysis and are very unpredictable, especially in bundles where the geometry of entrapped air is indeterminate.

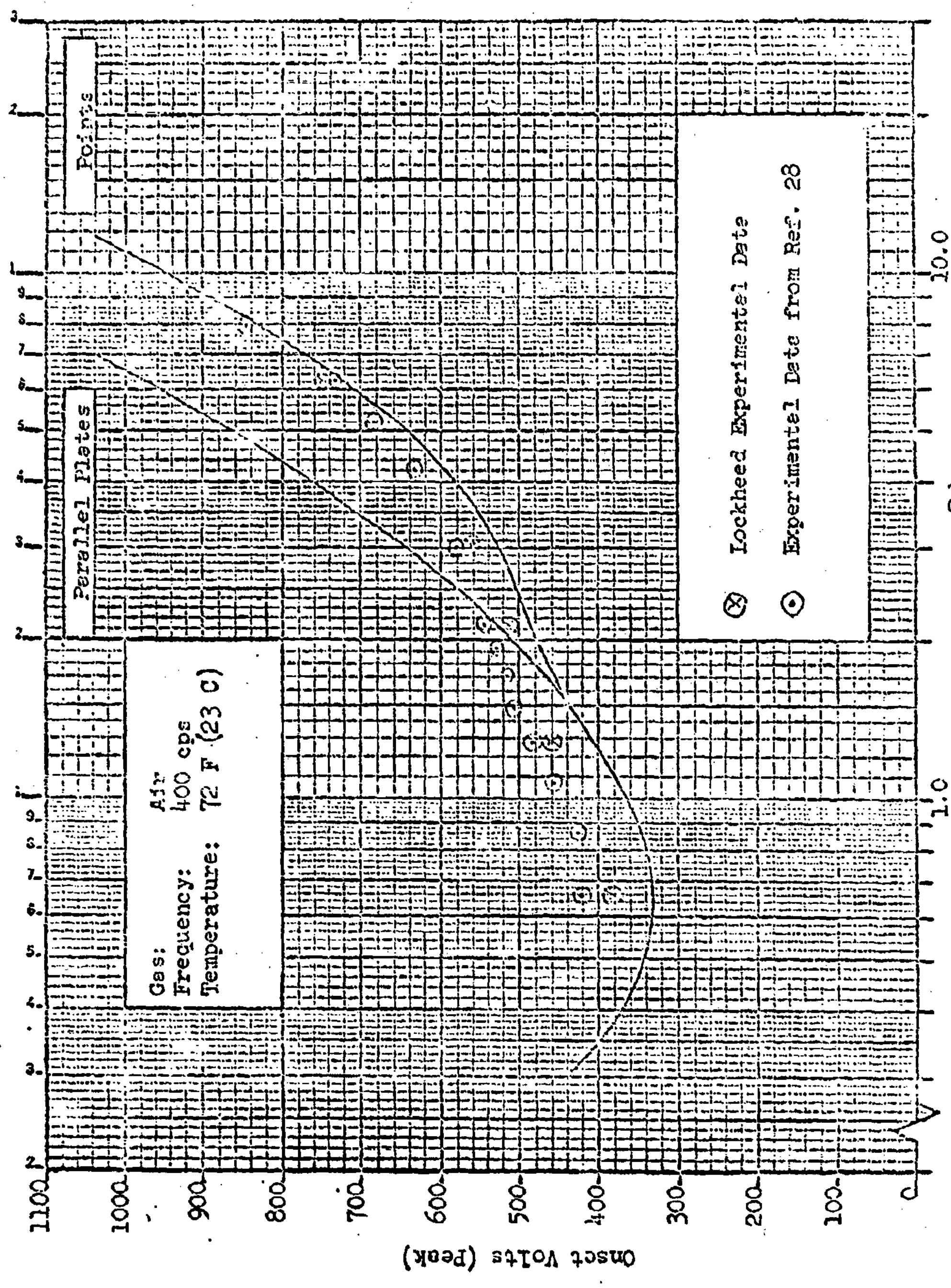

Figure 16 Comparison of Paschen curve of Figure 1 with behavior of needle-points of Figure 12d.

6.3 Reliability Aspects

The following is a list of desirable design factors for reliability concerning prevention or control over corona and sparkover in the SST environment:

1. Connectors and terminals should be completely enclosed to prevent moisture or contamination and a resulting reduction in breakdown voltage.

2. Special insulating techniques can be used which consist of placing the electrical wiring as close to electrical ground as possible and placing neutral wires between the phase wires; thus the voltage gradient is not between phases, but between phase and neutral.

3. The geometrical design of the electrodes, as well as the nature of their surfaces, can play an important part in facilitating lower breakdown voltages. Therefore geometrical irregularities such as sharp edges or points, which produce a local concentration in the electric field, should be avoided.

4. All exposed high voltage conductors should be coated or covered with dielectric material to eliminate the possibility of flashover, and to increase the voltage necessary for corona inception.

5. Supression devices, such as gas discharge tubes, should be considered to ensure that the maximum allowed transient voltages are never exceeded.

6. The use of sealed pressurized assemblies should be considered to eliminate the corona problem.

7. Some of the factors which lower the corona starting voltage are: decreasing the wire diameter; decreasing the wire spacing, but the effect of diameter change is much greater (standard wire of the same cross section as solid wire also has a lower corona starting voltage); decreasing the air density; increasing the air temperature (lowers air density); dirt, water, etc. on the conductor surface; physical surface conditions, such as nicks, pin points, etc.; and parallel magnetic fields.

7.0 FOLLOW-ON TEST PLANS

Plans for follow-on tests are described in Lockheed Report 19380. Tests will be conducted to verify design guidelines and safety factors for corona prevention using actual assemblies under realistic conditions. The plans include life test in repeated cycles on harness specimens, including wired connectors and termination assemblies. The tests will consist of application of normal and overvoltages at the operating temperature and altitude, observation of any corona or sparkover, immersion in water, normal disconnection and reconnection, vibration at room and elevated temperature, return to the temperature altitude chamber, and repetition of the cycle.

8.0 REFERENCES

1. E. V. Condon and Hugh Odishaw, Handbook of Physics, McGraw-Hill Book Company, Inc., New York, 1958, Section 4-6.

F. Llewellyn-Jones, Ionization and Breakdown In Gases, John Wiley and Sons Inc., New York, 1957, pp. 97, 113-127.

J. Roger Sheridan, A Study of AC Corona Voltage Levels, Boeing Airplane Company, Seattle, Washington, December 1956, Section VII.

2. A. L. Coats, "Performance of Electrical Connectors at High Altitude," AIEE Transactions, Vol. 79, Part 2, pp. 337-339, 1960.

L. B. Loeb, The Fundamental Process of Electrical Discharges In Gases, John Wiley and Sons Inc., New York, 1937, pp. 413.

W. P. Wallon, Connector and Cable High Altitude Performance Considerations, The Bendix Corporation, Scintilla Division, November 1962, pp. 3.

W. G. Dunbar, "Electrical Discharges at Altitudes Between 70,000 and 250,000 Feet," Supplement to IEEE Transactions on Aerospace, June 1965, pp. 242-246.

G. P. Thomson, Conduction of Electricity Through Gases, Cambridge University Press, London, England, 1928, Vol. 2, 3rd Edition, pp. 486.

G. Moses, Ruben Lee, and Robert J. Hillen, Insulation Engineering Fundamentals, Lake Publishing Company, Lake Forest, Illinois, 1958, pp. 7

Jaboc Millman, Vacuum-tube and Semiconductor Electronics, McGraw-Hill Book Company Inc., New York, 1958, Ch. 12, pp. 300.

3. Paul F. Stang, Extended Investigation of High Altitude Antenna Breakdown Phenomenon, "RF Corona on Titanium Surfaces at Elevated Temperatures up to 700 F," Part VIII, Lockheed Report 18481, December 1964.

Paul F. Stang, Extended Investigation of High Altitude Antenna Breakdown Phenomenon, "Corona Over Coated Titanium Surfaces", Part X, Sec. (a), Lockheed Report 19343, December 1, 1965.

4. United States Air Force, Air Research and Development Command, Air Force Research Division, Geophysics Research Directorate, Handbook of Geophysics, The Macmillan Company, New York, Revised Edition, 1961, Ch. 8.

5. Final Development Report for Dielectric Materials Ionization Study, General Electric Company, Schenectady, New York, June 1954, Ch. 10, pp. 31.

W. T. Starr, Dielectric Materials Ionization Study, General Electric Company, General Engineering Laboratory, Schenectady, New York, January 1954, pp. 1, 10, 12.

Paul F. Stang, Extended Investigation of High Altitude Antenna Breakdown Phenomenon "Humidity as a Factor in Corona and Breakdown", Part V, Lockheed Technical Manual 50175 - ARRD 6605, June, 1962.

Paul F. Stang, Extended Investigation of High Altitude Antenna Breakdown Phenomenon, "Humidity Effect at Low Air Pressure", Part VI, Lockheed Technical Manual 50295 - ARDD 6607, December, 1962.

Grahm Moses, Rueben Lee, and Robert Hillen, Insulation Engineering Fundamentals, Part II, Lake Publishing Company, Lake Forest, Illinois, 1958, pp. 9.

6. John C. Devins and A. Harry Sharbaugh, Electro-Technology, "The Fundamental Nature of Electrical Breakdown", February 1961, pp. 118.

Final Development Report for Dielectric Materials Ionization Study, General Electric Company, Schenectady, New York, June 1954, ch. 8, pp. 17-23.

7. SST Specification 422615, Generator System - Three Phase, 60 KVA.

8. R. L. McCartney, Electrical Cable Ratings for Supersonic Aircraft, Lockheed Report 19868, August 1966.

9. Grahm Moses, Reuben Lee, and Robert J. Hillen, Insulation Engineering Fundamentals, Part II, Lake Publishing Company, Lake Forest, Illinois, 1958, pp 9.

Final Development Report for Dielectric Materials Ionization Study, General Electric Company, Schenectady, New York, June 1954, Ch. 10, pp. 31-33.

W. T. Dakin, Westinghouse Engineer, "Physics of Insulation", May 1954, pp. 121.

10. H. J. Hoan, Corona Ignition and Extinction Voltage, Preliminary Data, DuPont Laboratories, Wilmington, Delaware, January 1966.

11. John C. Devins and A. Harry Sharbaugh, Electro-Technology, "The Fundamental Nature of Electrical Breakdown," February 1961, pp 112.

12. Murray Olyphant, Insulation, "Corona and Treeing Breakdown of Insulation Progress and Problems," Part I, February 1963.

13. Eugene J. McMahon, The Journal of Teflon, "Discharges on Teflon Resins," January 1961, pp. 7.

The Journal of Teflon, "The Effects of Radiation on Teflon Resins in Space," January 1961, pp. 6.

14. Gore Products and Services, " Corona Resistant Teflon", W. L. Gore and Associates, Inc., Newark, Delaware, pp. 8-10.

15. W. G. Dunbar, "Electrical Discharges at Altitudes Between 70,000 and 250,000 Feet", Supplement to IEEE Transactions on Aerospace, June 1965, pp. 242-246.

16. Rockbestos Aerospace and Electronic Wires and Cables, Rockbestos Wire and Cable Company, New Haven, Connecticut, 1966, pp. 10.

17. Teflon for Electrical and Electronic Systems, DuPont Company, Wilmington, Delaware, 1964, pp. 1-16.

18. C. G. Miller and Leonard B. Loeb, Journal of Applied Physics, "Negative Coaxial Cylindrical Corona Discharges in Pure N_2, O_2, and Mixtures Thereof", Volumn 22, Number 5, May 1951, pp. 614-621.

19. Paul F. Stang, Extended Investigation of High Altitude Antenna Breakdown Phenomenon, "Corona and Breakdown Tests", Part III, ARDD 6596, July 1960.

20. Paul F. Stang, Extended Investigation of High Altitude Antenna Breakdown Phenomenon, "Irradiation, Elevated Temperature and Pressurization", Part IV, Lockheed Technical Manual 50002 - ARDD 6600, December 1960.

21. Paul F. Stang, Extended Investigation of High Altitude Antenna Breakdown Phenomenan, "(a) Effect of Corona Reduction by Application of an Electrostatic Field, (b) HF Corona on Cables and Connectors", Part IX, Lockheed Technical Manual 50809, December 1964.

22. Paul F. Stang, Extended Investigation of High Altitude Antenna Breakdown Phenomena, "Characteristics of Voltage Breakdown and Corona Losses of High Altitude Aircraft Antennas", Part VII, Lockheed Technical Manual 50291 - ARDD 6607, July 1963.

23. The Journal of Teflon, DuPont Company, Wilmington, Delaware, June 1960, pp. 4-5.

24. William L. Greyson and Joseph I. LaSala, Properties of Various Wire and Cable Constructions Insulated with "H" Film, Tensolite Insulated Wire Company, Inc., Tarrytown, New York, December 1964, pp. 2-4.

25. T. W. Dakin, Electro-Technology, "Electrical Insulation Deterioration", December 1960, pp. 124-130.

26. H. P. Sparks, High Temperature Electrical Connectors, "Experimental Study of Visual Corona", Lockheed Memo Report, December 1965, pp. 54-84.

27. R. A. Noss, J. A. Hoffman, SST Wire and Wiring Components Development Program, Lockheed Report 19380.

28. J. Roger Sheridan, A Study of AC Corona Voltage Levels, Boeing Airplane Company, Seattle, Washington, December 1956, Section V.

APPENDIX A - REFERENCES

(A) John C. Devins and A. Harry Sharbaugh, Electro-Technology, "The Fundamental Nature of Electrical Breakdown", February 1961, pp. 104-122.

(B) John C. Devins and A. Harry Sharbaugh, Electro-Technology, "Electrical Breakdown in Solids and Liquids", October 1961, pp. 108-110.

APPENDIX A

A. THE NATURE OF ELECTRICAL BREAKDOWN IN AIR (Ref. A).

A.1 Behavior In a Uniform Field

Consider two electrodes in air, consisting of two flat plates with curved edges to produce a substantially uniform field, with a slowly rising DC potential between them. Electrons emitted from the cathode photo-electrically, or by other means to be discussed later, will be accelerated toward the anode, but will not travel far before encountering a gas molecule. If the energy of the electron is not too large, the collision will be elastic. The situation is analogous to a very samll ping pong ball striking a bowling ball. The electron may suffer very large changes in direction, but it will counce back with very little change of energy. The energy lost per collision is $2mM/(m + M)^2$ where m is the electron mass and M is that of the molecule. When $m \ll M$ this reduces to $2m/M$, which is approximately 10^{-3} to 10^{-5}.

The average distance an electron travels between collisions is the mean free path λ, and is dependent on the number of molecules per cubic centimeter, and the size of the molecules Θ (the electron size is negligible). The mean free path is given by:

$$\lambda = 1/n\Theta \qquad (1)$$

For a perfect gas, $n = 10^{20}$ P/T to within 5 percent, where p is the gas pressure (mmHg) and T is the absolute temperature. For air at one atmosphere

$= 5 \times 10^{-5}$ cm, and for air at 80,000 feet 20.874 mmHg and 600 F,

$= 4.0 \times 10^{-3}$ cm.

The electron makes more than $1/\lambda$ collisions in moving one centimeter across the gap, actually $\bar{c}/v\lambda$ collisions per centimeter of drift, where $\bar{c}$ is the average random velocity, and v is the drift velocity in the direction of the field. For air at one atmosphere this is about 3×10^5 collisions per centimeter.

Some electrons enter into the process of back diffusion. The electron suffers a series of collisions which returns it to the cathode. The probability of this occurrence depends on the applied field and the opposing electric field due to the charge on the electrons. When the voltage is near zero most of the electrons emitted return to the cathode. As the field is increased the current increases until few electrons return to the cathode. The current then approaches a saturation value which depends directly on the number of electrons emitted per second from the cathode.

The plateau value of current corresponds to the collection of essentially all of the electrons from the cathode. The further rise that occurs with still further increasing field is explained by consideration of the resultant inelastic collisions of electrons and molecules. In such collisions a large fraction of the electron's energy may be lost. However, energy can be transferred in collisions between an electron and a molecule only if the electron possesses at least the amount required to raise the molecule to a higher quantum level. Excitation of electrons to higher energy levels is a dominant energy loss mechanism. Such levels are separated by several electron volts, and this energy may reappear as light as the electron returns to its normal orbit.

When an electron possessing sufficient energy collides with a molecule, it may eject from the molecule another electron, and leave behind a positive ion. Each of the new electrons can itself be accelerated in the field to produce further ionization, and an avalanche of electrons finally reaches the anode. The positive ions move to the cathode and contribute to the total current in the gap, but they are unable to cause collisional ionization themselves. Because of their large mass they lose on the order of

half their energy on each elastic collision. Thus, the positive ions can never gain sufficient energy in the field at ordinary pressures to ionize another molecule.

The First Townsend coefficient, α, is defined as the number of ionizing collisions made by one electron drifting one centimeter in the direction of the field. The quantity $1/\alpha$ is the average distance in the field direction between ionizing collisions. That is:

$$\frac{di_e(x)}{dx} = \alpha i_e(x) \tag{2}$$

where X is the distance in the gap measured from the cathode, and $i_e(x)$ is the electron component of the current at X. Since equal numbers of positive ions and electrons are generated by collisional ionization:

$$\frac{di_+(x)}{dx} = -\alpha i_e(x) \tag{3}$$

The sum of the positive ion and electron currents will be the total current, i, as measured in the external circuit. Thus:

$$\alpha i_e(x) = i_e(o)\, \epsilon^{\alpha x} \tag{4}$$

where $i_e(o)$ is the electron current at the cathode. Substituting in (3) for the positive ion current and integrating:

$$i_+(x) = -i_e(o)\, \epsilon^{\alpha x} + A$$

where A is the constant of integration. The positive ions do not contribute to the current at the anode so:

$$i_+(\delta) = o$$

and,

$$A = i_e(o)\, \epsilon^{\alpha x}$$

where δ is the gap length. Therefore, the current which would be measured

by a meter in the external circuit is:

$$i = i_+(x) + i_e(x) = i_e(0)\, \epsilon^{\alpha x} \qquad (6)$$

Since α increases with the field, the collisional multiplication factor $\epsilon^{\alpha\delta}$ will increase very rapidly indeed with field.

The number of ionizing collisions per centimeter made by an electron moving through the gap will be proportional to the total number of collisions per centimeter times the probability that a collision will result in ionization. The total number of collisions is proportional to the gas pressure p, so α is proportional to the pressure. The probability of ionization depends on the electron energy. If the energy is less than the minimum amount required to eject an electron from a molecule, ϵ_i the probability is zero. Above this energy the probability increases, passing through a maximum when the energy is of the order of 10 x ϵ_i . At very high energies the probability of ionization decreases with decreasing interaction time.

Because of the many collision electrons experience in their travel across a gap, they will have a distribution of energies ranging from near zero to a value somewhat above ϵ_i. Energy is gained by the electrons in the field and lost by collisions. Except at extremely low pressures, the electrons will reach a steady state in energy within a very short distance after leaving the cathode. This means the rate of energy gain will just equal the rate of energy loss, and the energy distribution will be uniform throughout the gap. Thus, for an electron moving a distance ΔX in the direction of field E;

$$E \Delta X = V \Delta \epsilon \Delta X$$

where V is the number of collisions per centimeter of travel and $\Delta\epsilon$ is the average energy lost per collision. The number V is proportional to the product of the gas pressure, p, and the cross-section of the molecules. These cross-sections are determined by the electron energy. Also, $\Delta\epsilon$ is determined by the relative values of all cross-sections (excitation to various electronic states, ionization, etc.,) and so it too is a function of

electron energy. Thus, the above equation shows that the electron energy distribution will be a function of E/p.

To summarize, α is proportional to p and some function of E/p. The areas where the energy distribution curve overlaps the ionization probability curve determine α. For most gases the required experimental data are not available, although semi-emperical methods, discussed later are useful.

An increase in the collision cross-section will lower the electron energy distribution in the same manner as an increase in p (or decrease in E/p. Generally α will be decreased.

If the electrode spacing δ is changed, keeping α constant, a plot of the logarithm of the observed current against δ should give a straight line with slope α. Now it is expected that α/p equals $f(E/p)$, so α should remain constant if the field is kept constant. If the pressure and field is doubled the slope of the line is doubled.

Townsend found that above a certain sparking distance δ_S the current is independent of external illumination (of the cathode to cause emission of electrons). Some additional mechanisms are operative in the production of additional electrons at the cathode:

1. Ions striking the cathode cause the ejection of electrons.

2. The absorbed energy may appear as radiation of light as a result of the excited molecular electron falling back to its normal energy level. This radiation may fall upon the cathode to produce photo-emission of electrons.

3. Some of the electronically excited molecules may collide with neutral molecules to lose a small fraction of their energy. These metastable molecules may diffuse back to the cathode and cause electron emission on striking it.

These three processes are described quantitatively by a coefficient γ which is defined as the number of secondary electrons produced at the cathode per electron produced in the gap by primary collisional ionization. Although the magnitude of γ may be small (e.g. 10^{-4}), its overall effect may be large since these secondary electrons are produced at the cathode, and each will be multiplied by the factor $\epsilon^{\alpha\delta}$ (perhaps 10^{7} or more) by the time it crosses the gap.

The coefficient λ is not proportional to pressure, but is determined by the energy of the primary electrons, so it is a function of E/p.

The number of new electrons created per second by a current $i_e(x)$ in a small distance dx is $\alpha i_e(x)dx$; therefore, the total number of electrons generated in the gap per second is given by the integral:

$$\alpha \int_0^{\delta} i_e(x)\,dx$$

From the definition of γ and the use of Equation (4) the number of electrons produced at the cathode is:

$$\gamma \int_0^{\delta} \alpha i_e(x)\,dx = \gamma i_e(0)(\epsilon^{\alpha\delta} - 1)$$

Thus if i_o is the electron current at the cathode due to external illumination, the total electron current at the cathode, $i_e(0)$ becomes:

$$i_e(0) = i_o + \gamma i_e(0)(\epsilon^{\alpha\delta} - 1)$$

Rearranging and substituting in Equation (6), yields the total current which is measured in the external circuit:

$$i = \frac{i_o \epsilon^{\alpha\delta}}{1 - \gamma(\epsilon^{\alpha\delta} - 1)} \qquad (7)$$

This current becomes very large (limited only by the external series resistance of the power supply and the conducting gas) as the denominator of the preceding equation approaches zero, that is when:

$$\gamma\left(\epsilon^{\alpha\delta}-1\right) = 1 \tag{8}$$

or, since $\epsilon^{\alpha\delta} >> 1$, when,

$$\gamma\,\epsilon^{\alpha\delta} = 1 \tag{9}$$

Since $(\epsilon^{\alpha\delta}-1)$ is the number of electrons (or positive ions) generated by a single electron crossing the breakdown gap, and γ is the number of secondary electrons generated per primary electron in the gap, Equation (8) is satisfied, and breakdown occurs, if for each electron avalanche at least one secondary electron is generated at the cathode to initiate another avalanche, and the discharge becomes self-sustaining. The fulfillment of Equation (8) does not depend on the value of i_o provided there are sufficient electrons to start the sequence of avalanches. The variables are V_s and $p\delta$. Solving explicitly for the sparking potential gives:

$$V = \psi(p\delta)$$

where ψ is a function of the variable $p\delta$ only. This is the mathematical expression of Paschen's Law. E/p is the fundamental parameter determining the breakdown voltage if the temperature is constant so $E\lambda$ is proportional to E/p. If the temperature varies the fundamental variable becomes ET/p so, to include the effects of temperature, Paschen's Law should be expressed as:

$$V = \psi\left(\frac{p\delta}{T}\right)$$

where T is the absolute temperature. An alternative way of stating Paschen's Law is

$$V_s = \psi(n\delta)$$

where n is the number of molecules per cubic centimeter.

This is not a very stringent requirement since cosmic radiation and radiation from radioactive impurities are easily able to provide these initiating electrons.

The fulfillment of the breakdown criterion for a particular gap depends on γ and α. These variables depend on (E/p), gas pressure, the cathode composition (through γ) and the nature of the gas.

A.2 Paschen's Law (Ref. A)

As already shown, $\alpha/p = f(E/p)$ and $\gamma = g(E/p)$ By substituting into Equation (8) and setting the sparking potential V_s equal to $E_s \delta$ (valid for uniform fields) the following expression (valid at breakdown) is obtained.

$$g\left[\frac{V_s}{p\delta}\right]\left(\epsilon^{p\delta f(V_s/p\delta} -1)\right) = 1$$

A.3 Analytical Expression of Paschen's Law (Ref. A).

Consider an electron moving across a breakdown gap δ under the influence of an applied field E. It will undergo many collisions with gas molecules. Assume it has an average random velocity $\bar{c}$ and a smaller drift velocity v in the direction of E. Following its tortuous path, it will eventually gain the necessary energy ϵ_i to ionize a gas molecule by collision after it has traveled a net distance d_i measured along the direction of E. Due to its random motion the electron will have traversed a longer distance $\bar{c}\, d_i / v$ in the process of attaining the ionization energy. If the average number of collisions is λ, then the total number of collisions becomes $\bar{c}\, d_i / v\lambda$. If $\Delta\epsilon$ is the amount of energy lost per collision, then $\Delta\epsilon[\bar{c} d_i / v\lambda]$ is the total energy lost. If the electron proceeded across the gap without losing any energy, then $V d_i / \delta$ would be the energy gain from the field in traveling this critical ionization distance d_i. In order to produce ionization the electron must have a

net energy gain of at least ϵ_i , and so the following relation holds:

$$\frac{Vd_i}{\delta} - \frac{\bar{c}\, d_i \Delta\epsilon}{V\lambda} = \epsilon_i \tag{10}$$

By definition $\alpha = 1/d_i$ so:

$$\alpha \cdot \frac{1}{\epsilon_i}\left[\frac{V}{\delta} - \frac{\bar{c}\,\Delta\epsilon}{V\lambda}\right] \tag{11}$$

From Equation (9) the equation for breakdown is:

$$\alpha\delta = \ln\left(\frac{1}{\gamma}\right)$$

and, substituting for α and replacing V by V_S gives:

$$V_S = \epsilon_i \ln\left(\frac{1}{\gamma}\right) + \frac{\bar{c}\,\Delta\epsilon}{V}\left(\frac{\delta}{\lambda}\right) \tag{12}$$

The terms $\ln(1/\gamma)$ and $(\bar{c}\Delta\epsilon/V)$ usually do not vary strongly with (δ/λ) so, to a first approximation V_S is a linear function of δ/λ or $p\delta$ with an intercept of:

$$[\epsilon_i \ln(1/\gamma)].$$

The deviations of the calculated curve using Equation (12) from the observed values are due to small variation in γ, c, v, and $\Delta\epsilon$. However, all of these quantities are functions of $V_S/p\delta$ and, therefore, functions of at breakdown. Therefore, Equation (12) satisfies Paschen's Law since is purely a function of the variable $p\delta$.

This simple model is concerned with average quantities, and the equation loses its meaning when d_i becomes of the order of δ. For example, when this occurs, electrons make relatively few collisions in their transit across the gap, and as a result $\bar{c}$ and V become functions of electron position in the gap. In practice as $p\delta$ becomes sufficiently low, the sparking voltage traverses a minimum. This is expected on the basis of the Townsend Theory, since at very low pressures, the necessary number of ionizing collisions can be achieved only if the applied field is very substantially raised to increase the efficiency of the primary and secondary ionization processes.

From Equation (10) can be calculated the fraction of the energy gained from the field which is used in ionization (i.e., the ionization efficiency). For air at one atmosphere pressure and $\delta = 1$ cm, $\alpha\delta$ or δ/d_i has been measured to be about 19 at breakdown and $V_s = 30 \times 10^3$ volts. For oxygen and nitrogen respectively, $\epsilon_i = 13$ and 15 ev. Solving Equation (10) for the ratio of the second to the first term gives the ratio of energy lost to all processes other than ionization to that gained from the field. Substitution of the above numbers yields a value of about 99 percent, or only 1 percent of the energy gained by the electrons from the field is used in the ionization process, the remainder being dissipated as inelastic (excitation) and elastic (heat) collisions. A small fraction is lost by heating the anode; this amount becomes increasingly important at lower values of $p\delta$. Near the Paschen minimum ($p\delta = 0.7$ and $\alpha\delta = 3$) the ionization is much more efficient, approximately 20 percent of the energy gained by the electrons appearing in ionizing processes.

A.4.a <u>More Quantitative Breakdown Relation (Ref. A)</u>

Reference to Paschen's Curve (Figure A.1) shows that at low pressures a long gap may break down at a lower voltage than will a short gap at values of $p\delta$ to the left of the minimum.

The expression for α/p as a function of E/p is shown in Equation (11) on the basis of a very highly oversimplified model. For practical use we must have a more quantitative relationship between these two quantities. The energy distribution function $W(\epsilon)$ for electrons and the probability of ionization $P_i(\epsilon)$. Theoreticians have computed $W(\epsilon)$ by equating all possible ways for dissipating energy (elastic and inelastic collisions) to that gained from the field. The function $P_i(\epsilon)$ is measured experimentally and its product with $W(\epsilon)$ gives the desired quantitative expression for $\alpha/p = f(E/p)$. No single equation is valid for all ranges of E/p, but an expression useful over a large range of practical value is:

$$\frac{\alpha}{p} = A\,\epsilon^{-\beta p/E} \qquad (13)$$

where A and B are constants characteristic of a particular gas. Inserting Equation (13) into the Townsend criterion for breakdown (Equation (8)), gives a useful quantitative expression for the sparking potential as a function of $p\delta$ as follows:

$$V_s = \frac{Bp\gamma}{\ln p\delta + \ln\left[\frac{A}{\ln(1+1/\gamma)}\right]} \qquad (14)$$

Under practical conditions, the change in γ with $p\delta$ is small and the logarithmic dependence reduces it even more; hence the term in the brackets is often treated as a constant.

The dashed line of Figure A.1 has been computed using Equation (14) where, from measurements of α/p vs E/p, A = 8.8 cm^{-1} $mmHg^{-1}$ and B = 256 $volts^{-1}$ cm x mmHg. By fitting the equation to the experimental data at $p\delta$ = 0.7 mmHg x cm, γ is found to be 4.9×10^{-4} the agreement with experimental values (the circles) is seen to be much better than that obtained with the simplified expression.

A.5 Time Lags (Ref. A)

When a field sufficiently large to cause breakdown is applied there are two reasons why sparkover does not occur immediately: (1) the time required for one or more initial electrons to appear in a favorable position in the gap to lead to the necessary avalanches, and (2) the development of these avalanches and build-up of current to a value corresponding to breakdown requires time because of the finite mobilities of the particles.

These time lags are not significant to the problem of corona and sparkover in the SST power system wiring. They are very short, on the order of 100 microseconds or less, reduced typically to less than 10 microseconds at two percent overvoltage above the minimum sparking potential for a set of conditions.

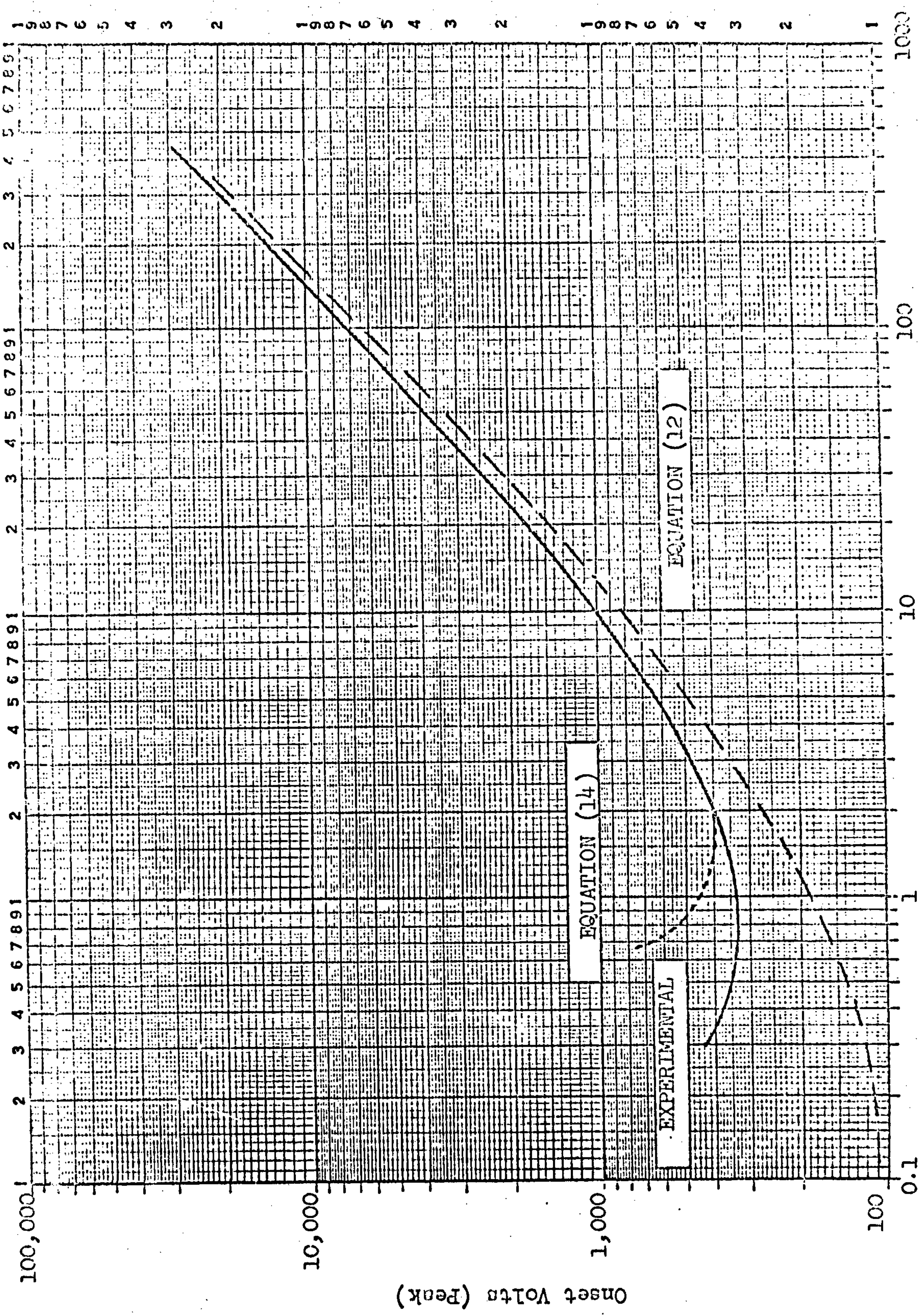

FIGURE A.1. EXPERIMENTAL AND THEORETICAL PASCHEN CURVES

A.6 Breakdown in Inhomogenous Electric Fields (Ref. A)

The preceding discussion has been concerned exclusively with uniform electric fields in which E is constant and independent of X where X is the coordinate along the drift path of an electron participating in the breakdown process. This condition is readily fulfilled with parallel-plate electrode systems having contoured edges, and for two similar spheres which are separated by less than one-tenth of their diameter. Configurations commonly encountered in practice generate inhomogeneous fields. Examples are widely spaced spheres or cylinders and sphere-to-plane. Effort is expended in electrical design to reduce the field inhomogeneity to a minimum.

For such electrode systems, α is a strong function of E so $\alpha\delta$ must now be replaced by $\int_0^\delta \alpha\, dx$. The Townsend criterion for breakdown is a nonuniform field then becomes:

$$\gamma\left[\exp\left(\int_0^\delta \alpha\, dx\right) - 1\right] = 1$$

The integral $\int_0^\delta \alpha\, dx$ is not generally a function of the product $\alpha\delta$ and Paschen's Law is no longer valid. Although Paschen's Law is not applicable to electrode systems which give rise to inhomogeneous fields there is a much more general "Law of Similitude" which does apply to both uniform and nonuniform field geometries. Paschen's Law is a special case of this more general law and applies only to uniform fields.

In addition to knowing E = f(X) in order to apply Equation (17) the functional dependence of γ and α upon E must be known. This dependence has been measured experimentally for a number of gases. The sparking potential computed by Equation (17) agrees well with observed values for moderately inhomogeneous fields. However if (dE/dx) is very large the electron velocity will be changing rapidly and will not be characteristic of the value of E in the region of the gap in question, i.e. the electrons lag behind the field. If the anode is small compared to the electron mean free path the electrons may not strike it following their last collision with a gas molecule. As a result extra ionization may be possible. For asyrometric

electrodes γ will depend on the polarity of the electrodes. Usually γ is larger with the smaller electrode as the cathode and a lower value of results.

A.7 The Law of Similitude

The volt-ampere characteristic of a given gas discharge will not change if all linear dimensions are increased by a constant factor and the gas pressure is reduced by the same factor.

A.8 Inhomogeneity Due to Space Charge

Poisson's equation demands a change in field strength across a gap even though the space charge is uniformly distributed:

$$E(x) = E_{APP.} + 4\pi\rho\left(\frac{\delta}{2} - x\right)$$

where ρ is the net charge per unit volume.

A.9 Thermionic Emission

At sufficiently elevated temperatures thermionic emission may occur from the cathode in the range of 1000 to 2000 K and reduce the breakdown voltage. The temperature at which this occurs will be determined by the thermionic work function of the cathode.

Thermal ionization of the gas occurs in the range of 2000 to 5000K - too high for consideration in the wiring system problem.

A.10 Corona Stabilization

If the field is generated by very asymmetrical electrodes it is possible to obtain localized breakdown which does not bridge the gap. This is corona and it is self-sustained. Complete breakdown occurs at still higher voltages. Invariably both the flash-over and the corona onset voltages will be lower than for uniform fields.

A.11 Breakdown Under Alternating Fields

At sufficiently low frequencies breakdown occurs when the peak value of the a-c voltage reaches the d-c value predicted by the Townsend Criterion. A decrease in the sparking potential occurs if the period of the applied voltage is comparable to the transit time of the charged carriers. This occurs at frequencies too high to apply to the wiring system problem.

A.12 Influence of Molecular Structure

Since in the Townsend Criterion γ is a pre-exponential factor while α appears as an exponent the electric strength is much more sensitive to the value of α than to that of γ.

Using certain assumptions, α may be calculated as a function of E/p in terms of the molecular parameters. It has the form:

$$\frac{\alpha}{p} = A\,\epsilon^{-\beta p/E} \qquad \text{(See Equation 13)}$$

in which,

$$\beta = K(\sigma_0\,\theta)^{1/2}(\epsilon_i - \epsilon_o)^{3/2} \qquad \text{(See Equation 14)}$$

where θ is the elastic cross-section; σ the inelastic cross-section for electronic excitation expressed as:

$$\sigma = \sigma_0(\epsilon - \epsilon_e)$$

and ϵ_e is the lowest energy of the electrons at which excitation can occur.

A.13 Representation of a Void (Ref. B)

Let us consider the model for a dielectric containing a void shown in Figure A.2(a). Here, C_v represents the capacity of the void which is in series with a solid dielectric whose capacity is C_s, and C_d represents the capacity of the remaining solid in parallel with the combination. If a sinusoidal voltage, V, is now applied to the system, the voltage will divide capacitively between C_v and C_s - providing the electric strength of the gas in C_v is not exceeded and no discharges occur.

The electric strength of a gas is relatively independent of the nature of the electrode material. It has been found that even when the electrodes consist of a typical solid dielectric, the sparking potentiol, V_s, differs little from that for most metal electrodes. Thus, when the voltage across the void V_t (Figure A2(b), reaches V_s, breakdown will occur. Charge produced by ionization in the gas in C_v will remain on the insulating surfaces of C_v to lower its potential to V_e, the extinction voltage for the discharge. At the same time, charge will flow from the external circuit (including C_d, if the external circuit impedence is sufficiently high) to raise the voltage across C_s. The discharge time is very short - perhaps 10^{-7} sec - and can be related to the transit times of ions and electrons in the discharge. After the fast discharge, the voltage on C_v continues to rise at the sinusoidal rate until, after an increase of V_e, a further discharge can occur. These will continue to the neighborhood of the peak of the applied voltage, after which the voltage across C_v will decrease and discharges will cease. The charge remaining on C_v will augment the applied field on the next half cycle, and a new series of discharges will begin at an earlier point. This may occur even at the zero of applied voltage, as shown in Figure A.2(b) or before or after the zero - depending upon the amount of charge deposited. This, in turn, is a function of how much the peak voltage exceeded the starting voltage in the first half-cycle. As a result, more discharges will occur on the second half-cycle. After several half cycles, a steady state will, of course, be reached at which time the average charge transported on each half-cycle will be the same. At this time, if the peak applied voltage is increased, discharges will begin sooner on the voltage wave and the number of discharges per half-cycle will increase.

An interesting feature of this model is that it permits an explanation of the often-observed intermittent discharges which may appear for many cycles and then cease. Thus, even if the peak applied voltage is somewhat below that required for sustained discharges, it may be augmented by the field due to charge deposition by a chance discharge (owing, for example, to a fluctuation in voltage) so that a further breakdown can occur. Discharges may then continue on each half-cycle - but, as a little reflection will show, at an

earlier point on the wave for each cycle. Eventually, the sum of the applied voltage and that due to deposited charge will fail to reach the sparking potential on a half-cycle, and discharges will cease. The phenomenon will be accentuated for low values of the extinction voltage V_e.

A number of studies have been made of the so-called "epochs" of the discharges on the voltage wave, and on the basis of these observations, the general validity of the above simple model has been confirmed. Detailed considerations suggest, however, that some modifications are necessary. It has been found, for example, that - except perhaps for voids of very small cross section - the whole void is not discharged. Only relatively small areas appear to be involved in each discharge, and it seems likely that the extinction voltage is low. As a result, sites once discharged tend to remain in such condition for a relatively long time, changing slowly as transverse leakage occurs.

For d-c stresses, the model of Figure A.2(a) predicts that discharges can occur only as the voltage is raised. In practice, of course, C_s will always possess a leakage resistance, R_s, effectively in parallel with it, so that the voltage across C_v can build up again with a time constant R_sC_s. Thus, depending upon the magnitude of the applied voltage and this time constant, recurring discharges in voids will occur even with d-c voltages. For most good dielectrics, however, R_sC_s is very long and damage due to discharges is usually much less with d-c than with a-c of comparable stresses.

The application of the model of Figure A.2(a) to practical systems is further complicated by the fact that such systems seldom contain only one void. There is usually a wide distribution of void sizes and, in the case of an electrode on the dielectric surface, an essentially infinite distribution of air gaps is available at the electrode edge. Let us consider, for example, a sphere resting on a sheet of dielectric of thinckness δ', and let us assume as a first approximation that the field in the varying gap is uniform normal to the dielectric. Our model must now be replaced by one containing a large number of series combinations of C_v and C_s, each C_v corresponding to a different air gap Now, the voltage across any particular air gap is $V_a = V(C_s/(C_v + C_s)$

where V is the applied voltage. Assuming the thickness of the dielectric remains constant, this may be written:

$$V_a = \frac{V}{1 + \frac{\delta'}{\epsilon\delta}}$$

where ϵ is the dielectric constant of the solid and δ is the air gap uncer consideration. Now, if V is raised until the peak value V_i is just that required to initiate stable discharges, V_a must be equal to V_s, the sparking potential. Thus from a knowledge of V_s as a function of δ, we can calculate the discharge initiation voltage, V_i, often referred to as the corona starting voltage.

Let us assume, for example, that in the range of void sizes of interest:

$$V_s = A\delta + B$$

Then,

$$V_i = \left[\frac{\delta'}{\epsilon\delta} + 1\right](A\delta + B)$$

It is interesting to note that this expression for V_i has a minimum value with varying δ. Discharges will therefore first appear at this value of δ and with this value of V_i. Curves for V_i as a function of δ for various values of δ'/ϵ are shown in Figure A.3 for air. These curves were plotted using measured data for V_s as a function of δ, rather than the simplified expression assumed above. It should be noted that the minima in this figure bear no relation to the Paschen law minimum, except when δ'/ϵ is zero. On the contrary, as seen above, they appear even when a linear relationship between V_s and δ is assumed. Figure A.3 is useful for calculating V_i from knowledge only of the dielectric constant and thickness when a wide range of void sizes or an electrode edge are present as is often the case in practical systems. It has been found to apply remarkably well for all geometries except the sharpest-edged electrodes, where field inhomogeneities must be taken into account.

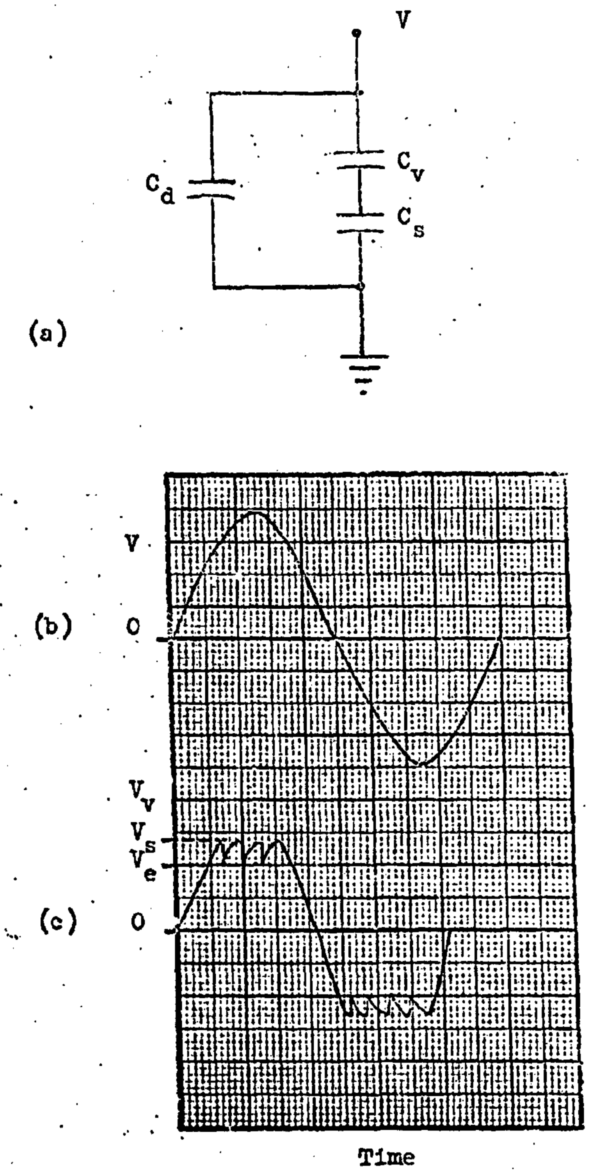

FIGURE A.2 (a) Equivalent circuit of a dielectric containing a void.
(b) Time dependence of applied voltage V.
(c) Time dependence of void voltage V_v.

A number of discharge detectors and devices for measuring energy dissipated in the discharges are available, but more than a cursory examination of them is beyond the scope of this report. They include devices based on optical techniques (e.g., photomultipliers), aural methods (microphones), high-frequency electrical detectors (tuned circuits and amplifiers as well as radio receivers), and various types of bridges designed to measure electrical losses. The last two have enjoyed the most popularity in recent years.

Since the discharges are of very short duration, the spectrum of their Fourier components extends well into the megacycle range and they are readily isolated from the power-frequency currents. As a result, very high gains are possible, and detection of discharges containing only a few electron avalanches is possible. In some ways this has been unfortunate, since no one has as yet established the lower limit of discharge magnitude below which the life of commercial equipment is adequate. With the advent of more and more sensitive detectors, equipment which was earlier thought to be free of discharges has come under suspicion. Particular care must be taken under these conditions to eliminate stray discharges generated on the leads or in the power supply. Much remains to be done before reliable correlations between discharge magnitude and life of insulation are established.

Low-frequency bridges are corona detectors of relatively low sensitivity, since they measure the ratio of in-phase to out-of-phase current. However, they have the advantage of providing a direct measurement of the average energy dissipated in the discharges, a quantity which has in some cases been correlated with chemical degradation. A useful variation of conventional bridge techniques is one in which the charge, rather than the current, flowing to the system is measured as a function of the sinusoidally varying voltage. These may be plotted as a cyclogram on the oscilloscope, the area of which is proportional to the power dissipated.

Although time-consuming, perhaps the most direct method for evaluating the effects of discharges on electrical insulation is the measurement of the time-to-failure as a function of applied voltage. The fact that such a curve appears to approach infinite life asymptotically to the discharge

inception voltage is good evidence that failure is caused by discharges. The time required to establish such curves may be considerably reduced by increasing the frequency of the applied voltage. Provided that the normal a-c losses are sufficiently low so as to avoid dielectric heating, the frequency may be raised to as high as 1 mc without obtaining appreciable general heating of the dielectric by the discharges. It has been found that the rate of damage due to discharges is accelerated proportionally to the increase in frequency. This is not unexpected when one notes that, according to the model of Figure A.2(a), the total charge transferred by discharges per half cycle is a function only of the difference between the peak applied voltage and the voltage at which discharges are initiated. Thus, the total charge transferred per unit time should be proportional to the frequency of the applied voltage.

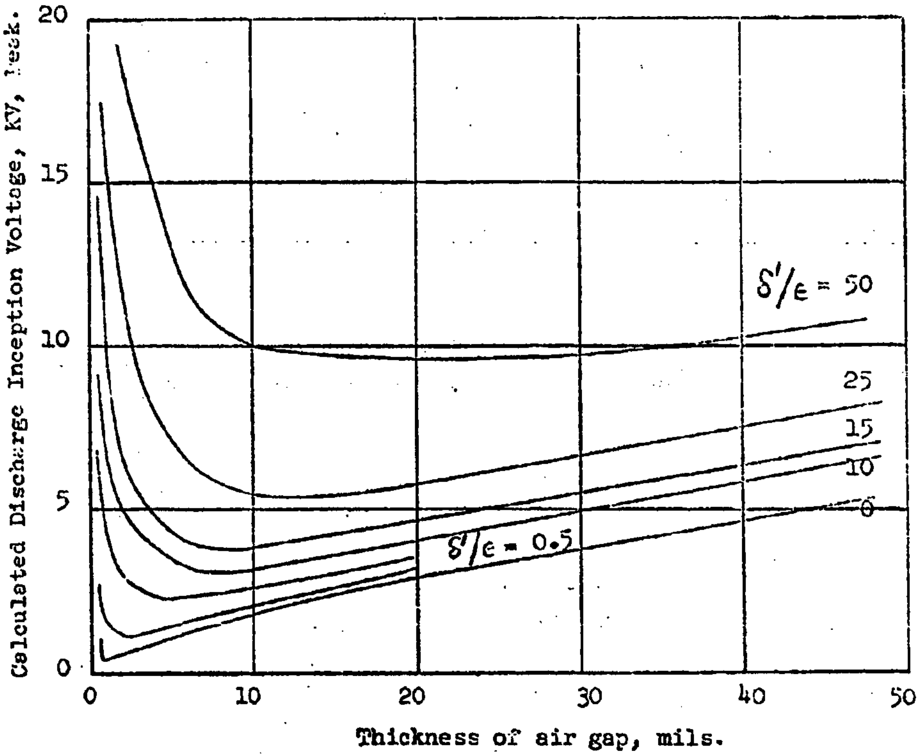

FIGURE A.3. Discharge inception voltage as a function of depth of void for various values of δ' / ϵ mil.